Palaeontology
The Palaeontological Association
www.palass.org

[Palaeontology, Vol. 63, Part 6, 2020, pp. 919–939]

BIOMECHANICAL PROPERTIES OF THE JAWS OF TWO SPECIES OF *CLEVOSAURUS* AND A REANALYSIS OF RHYNCHOCEPHALIAN DENTARY MORPHOSPACE

by SOFIA A. V. CHAMBI-TROWELL[1], DAVID I. WHITESIDE[1,2], MICHAEL J. BENTON[1] *and* EMILY J. RAYFIELD[1]

[1]School of Earth Sciences, University of Bristol, Bristol, BS8 1TF, UK; sc14927@bristol.ac.uk, mike.benton@bristol.ac.uk, e.rayfield@bristol.ac.uk
[2]Palaeontology Section, Earth Science Department, Natural History Museum, Cromwell Road, London, SW7 5BD, UK; david.whiteside@bristol.ac.uk

Typescript received 12 January 2020; accepted in revised form 15 April 2020

Abstract: Rhynchocephalians were a successful, globally distributed group of diapsid reptiles that thrived in the Mesozoic. Multiple species of *Clevosaurus* existed worldwide in the Late Triassic and Early Jurassic, characterized by shearing bladelike teeth perhaps functionally analogous to the carnassial teeth of mammals. Morphometric analysis shows that the dentary morphospace of clevosaurs differs significantly from that of other rhynchocephalians. Five *Clevosaurus* species occupied islands in the Bristol Channel archipelago of the UK, but generally not those occupied by mammaliaforms, suggesting dietary character displacement. Identifying the diet of such ancient, small tetrapods has been difficult. To identify the nature of their feeding mechanics and ecology, we apply finite element analysis to two near complete three-dimensional skulls of the species *Clevosaurus hudsoni* and *Clevosaurus cambrica* to estimate bite force, resistance to bending and torsion and the distribution of stresses in the jaws during biting. Both species had bite forces and tooth pressures sufficient to break apart chitin indicating that, like early Mesozoic mammaliaforms, clevosaurs could feed on tough-shelled beetles and possibly small vertebrates. In addition, the mechanical advantage of the jaws falls within the range of early mammaliaforms, so though we cannot demonstrate niche partitioning between members of the two clades, it raises the prospect that they may have been functionally similar.

Key words: Sphenodontia, Rhynchocephalia, *Clevosaurus*, biomechanics, bite force, finite element analysis.

CLEVOSAURUS is a genus of Sphenodontia that had near global distribution, with fossils of ten named species found in the Americas, Europe, Asia and Africa (Jones *et al.* 2013; Hsiou *et al.* 2015; Herrera-Flores *et al.* 2018). Sphenodontia is an infraorder of Rhynchocephalia, which with Squamata (lizards and snakes) comprises Lepidosauria, a clade that diversified through the Triassic. *Clevosaurus* species are notable for their mesiodistally elongated teeth which occlude precisely, leaving conspicuous wear facets on the opposing surfaces of the dentary and maxilla, and acting as a self-sharpening cutting surface (Whiteside 1983; Whiteside & Duffin 2017).

The blade-like teeth of *Clevosaurus* may have been functionally analogous to the shearing carnassial teeth of mammals (Whiteside 1983; Jones 2008). The species of *Clevosaurus* occur at the same time as the first mammaliaforms (Kielan-Jaworoska *et al.* 2004) and it has been suggested that mammaliaforms may have displaced sphenodontians, such as *Clevosaurus*, where they coexisted (Whiteside *et al.* 2016, 2017; Whiteside & Duffin 2017). Early mammals such as *Morganucodon* did not have carnassials, but they did have molars that shear-cut (Jäger *et al.* 2019) in similar fashion to those of insectivorous modern bats (Santana *et al.* 2011). They also had a notch at the base of their teeth, 'not quite a carnassial notch, but similar' (Pamela Gill, pers. comm. 2019). The diet of *Clevosaurus* remains uncertain, with suggestions ranging from herbivory (Fraser & Walkden 1983; Fraser 1988), to facultative omnivory (Fraser & Walkden 1983; Jones 2009) and faunivory (Fraser 1988; Jones 2008; Meloro & Jones 2012; Whiteside *et al.* 2017). Furthermore, the extent of dietary overlap and/or dietary displacement of clevosaurs by insectivorous mammaliaforms has not been assessed. The diets of the Early Jurassic mammaliaforms *Morganucodon* and *Kuehneotherium* have been identified as hard-shelled and soft-shelled insects respectively based on the application of lever mechanics, beam theory, finite element analysis (FEA) and tooth microwear analysis (Gill

doi: 10.1111/pala.12493

et al. 2014). Without a similar study of the ubiquitous *Clevosaurus*, the possibility of dietary ecological displacement cannot be tested.

Here, we calculate, compare, contrast and discuss the biomechanical properties of the teeth and mandibular rami of two species of *Clevosaurus* from the British Isles: *C. hudsoni* and *C. cambrica* (Figs 1, 2). We also explore morphological disparity of the dentary in relation to rhynchocephalian phylogeny. We compare the fossil taxa with extant *Sphenodon* because its mandibular morphology converges on the same morphospace as *Clevosaurus* (Herrera-Flores *et al.* 2017). Biomechanical properties considered here are maximum bite force, mechanical advantage, resistances to torsion and bending, and FEA of the distribution of stress in the mandibular ramus during biting. Taken together with the morphometric study, we use these biomechanical metrics to test whether *Clevosaurus* feeding mechanics and diet was convergent on that of coeval mammaliaforms.

Institutional abbreviations. AUP, Aberdeen University Palaeontological Collection (School of Geosciences), UK; MCN, Museu de Ciências Naturais, Fundação Zoobotânica do Rio Grande do Sul, Brazil; MCZ, Museum of Comparative Anatomy, Harvard University, USA; NHMUK, Natural History Museum, London, UK; NSM, Nova Scotia Museum, Halifax, Canada; SAM, Iziko South African Museum, Cape Town, South Africa; UFRGS, Universidade Federal do Rio Grande do Sul, Porto Alegre, Brazil; UMZC, University Museum of Zoology, Cambridge, UK.

METHOD

Specimens and taxonomy

Ten species of *Clevosaurus* are recognized worldwide. Five species are found in the UK; four in the Upper Triassic and one in the Lower Jurassic. Here we focus on *Clevosaurus hudsoni* (NHMUK PV R36832; Fig. 2A, B) from Cromhall Quarry in south-west England, and *C. cambrica* (NHMUK PV R37014; Fig. 2C, D) from Pant-y-ffynnon Quarry in southern Wales. We use digital 3D segmentation of the skulls of both taxa, as featured in O'Brien *et al.* (2018) and Chambi-Trowell *et al.* (2019). For details of the 3D reconstruction of both skulls, refer to Chambi-Trowell *et al.* (2019). We used the same CT datasets (for further information about the CT scans, see Chambi-Trowell *et al.* 2020, A) to further isolate the mandibular rami of each taxon in Avizo 8.0 (Visualization Sciences Group), then repaired damaged bone by using the Avizo interpolation tool to infill cracks and breaks and remove segmentation artefacts.

Note that the skull assigned here to *Clevosaurus hudsoni* has some unusual anatomical features that suggest its morphology is more similar to the syntypes discovered by Swinton (1939) than the specimens of a different morphotype described by Fraser (1988). Herein, we refer to NHMUK PV R36832 as *C. hudsoni*X.

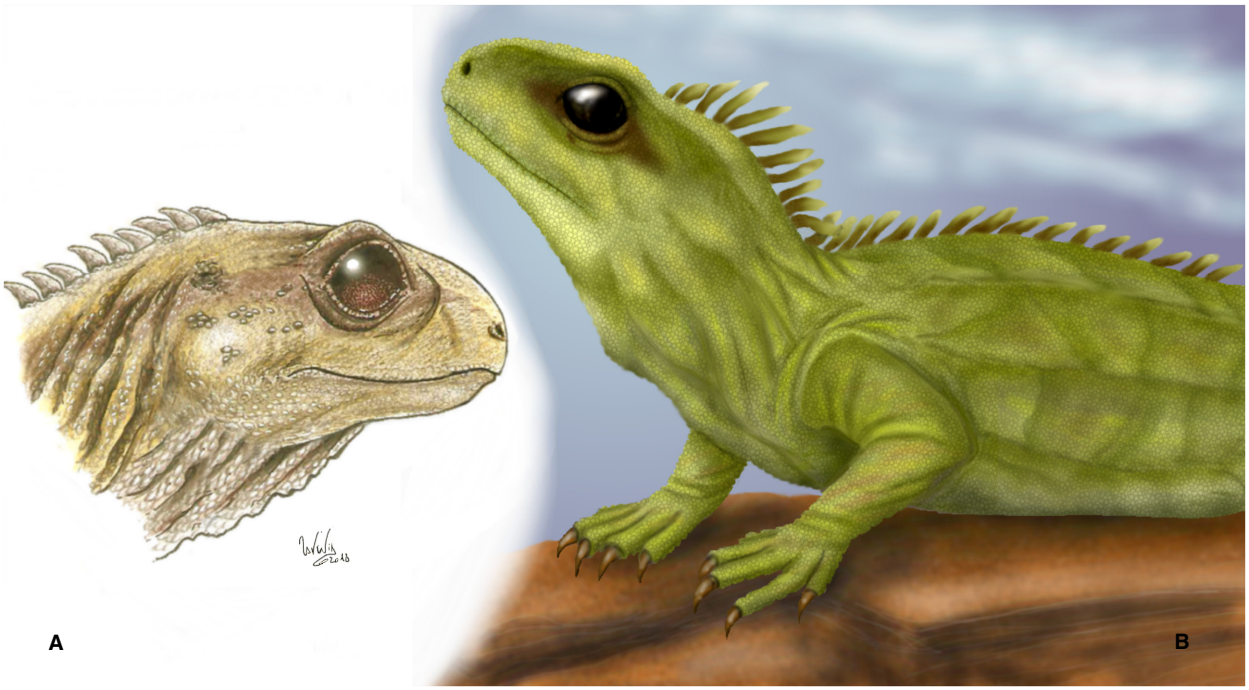

FIG. 1. Life reconstructions of *Clevosaurus*. A, *Clevosaurus hudsoni*X (modified from Lavinia Gandolfi, in Chambi-Trowell *et al.* 2019) based on NHMUK PV R36832. B, *Clevosaurus cambrica* (artist: Sofia Chambi-Trowell) based on NHMUK PV R37014. Colour online.

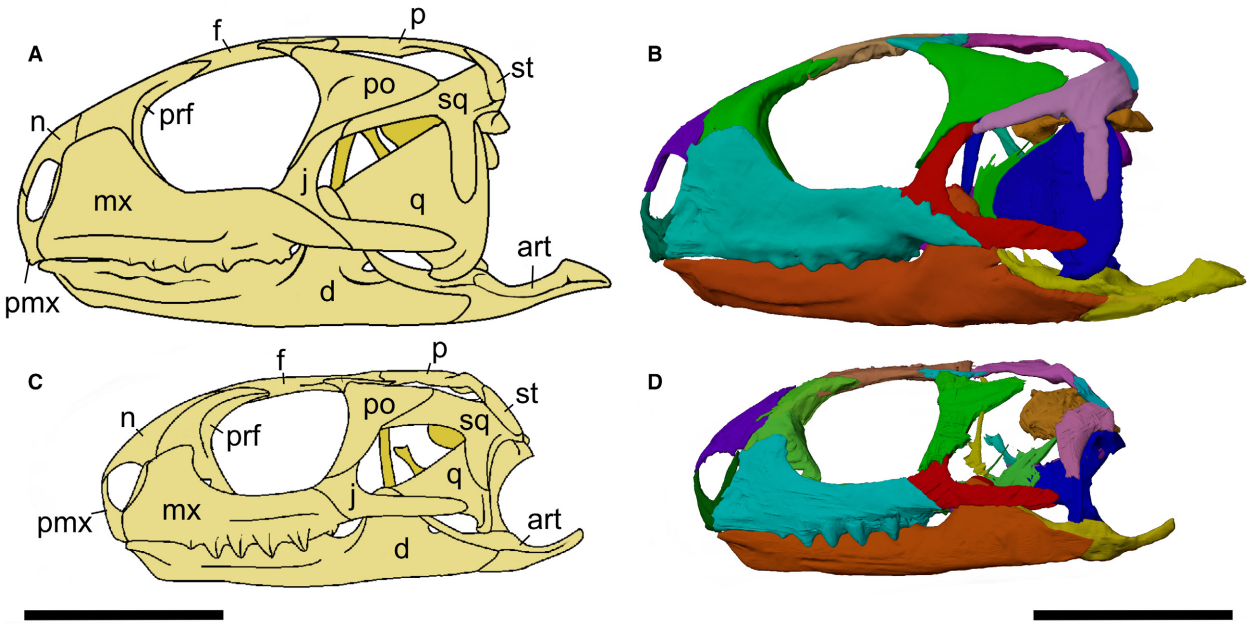

FIG. 2. The reassembled and reconstructed skulls of *Clevosaurus*. A–B, *C. hudsoni*X (NHMUK PV R36832). C–D, *C. cambrica* (NHMUK PV R37014). *Abbreviations*: art, articular complex; d, dentary; f, frontal; j, jugal; mx, maxilla; n, nasal; p, parietal; pmx, premaxilla; po, postorbital; prf, prefrontal; q, quadrate; sq, squamosal; st, supratemporal. Scale bars represent 10 mm. Colour online.

In addition to the two *Clevosaurus* species, we also included *Sphenodon* for comparison (Maisano 2001).

Adductor musculature

The two skull surface .stl files were individually imported into Avizo where they were converted into a solid volume and minor repairs were made to the bones around the adductor chamber; for example, in *C. cambrica* (NHMUK R37014) the supratemporal bar is incomplete. Following the methodology of Lautenschlager (2013), an adductor muscle reconstruction was then initiated by recognition of muscle attachment sites (Fig. 3) from osteological correlates where possible and, in their absence, by comparison with *Sphenodon* for which the adductor muscles are well documented by Jones *et al.* (2009). Relative muscle positions were then inferred using point-to-point connections, by selecting the sites of insertion and attachment, then using the Avizo interpolation tool.

We assume that the eight adductor muscles involved in the closing of the jaws are the same as those of *Sphenodon* (Curtis *et al.* 2009). Once all muscles were positioned so that they did not intersect with one another or with bone, they were built up, first using more point-to-point connections, then by increasing their volume gradually until it was constrained either by the skull itself or by the positions of neighbouring muscles (Fig. 4A–C, E–G). The exception to this is the pterygoideus typicus (mPtTy), for which much of the volume is not constrained by the skull or other muscles, being located beneath the mandible. For this muscle, two alternative volumes were tested (Fig. 4D–G), a moderately sized mPtTy where all the muscle falls roughly between the points of origination and insertion (Fig. 4D, F), and a second mPtTy that was increased in volume to match the size of this muscle seen in ventral view in *Sphenodon* (Jones *et al.* 2009) so that the medial edges of the muscle come close to the tubercles of the basioccipital (Fig. 4E, G). It is likely that in *Clevosaurus* the mPtTy would have had a relatively greater influence on bite force than in *Sphenodon*, because *Clevosaurus* had relatively smaller adductor chambers as a result of a more anteriorly placed braincase and the lack of a parietal crest. Furthermore, *Clevosaurus* has a greater region for muscle attachment on the articular, which is greatly truncated in *Sphenodon*. Reference was made throughout the reconstruction process to the adductor musculature of *Sphenodon* (Gorniak *et al.* 1982; Jones *et al.* 2009).

Bite force

Using the reconstructed skulls and musculature of *C. hudsoni*X and *C. cambrica*, muscle volumetric values, angles of insertion, muscle fibre-length and moment arm distances (distances between the articular condyle with teeth and adductor musculature) were calculated in Avizo using the 3D ruler tool (for measurements, see Chambi-

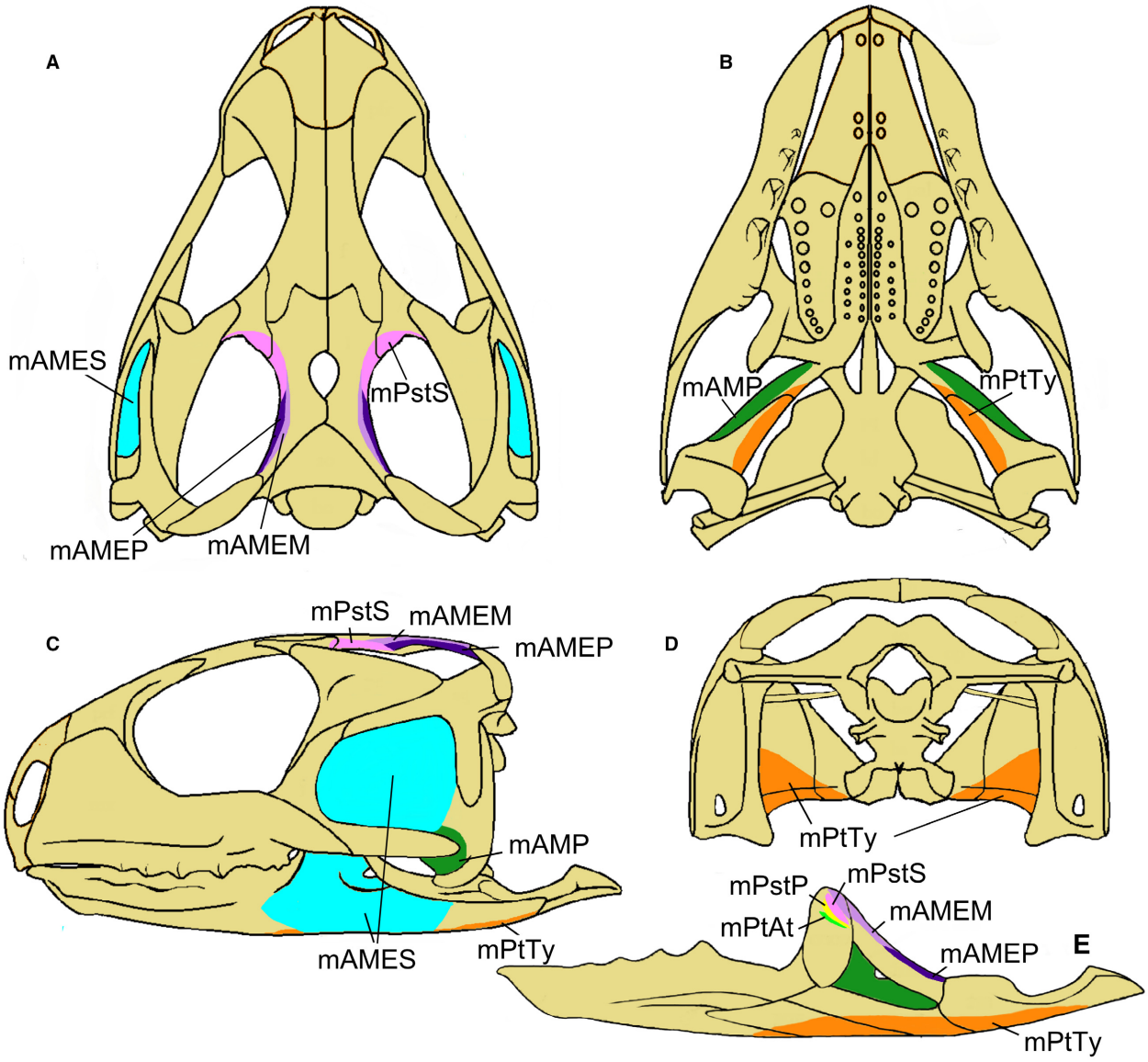

FIG. 3. Muscle attachment sites on the cranium of *Clevosaurus hudsoni*X (NHMUK PV R36832) in: A, dorsal; B, ventral; C, lateral; D, posterior view. E, mandible in lingual view. Colour online.

Trowell *et al.* 2020, tables S1–S2). Angle of insertion and muscle fibre length were calculated as averages of ten measurements taken at equal distances across the muscles, to account for differences over each muscle (with muscle fibre length = total length of muscle). Muscle moment arms were measured to the approximate central point of insertion for each of the muscles. For the mPtTy, two sets of 15 measurements were taken because this muscle has an extensive site of insertion that extends over both sides of the articular condyle and to account for wrapping of the muscle around the dentary. The first measurement was between the quadrate and the medio-ventral portion of the site of insertion on the dentary, and the second between the medio-ventral to lateral-ventral extent of the site of insertion on the dentary. Angles of muscle insertion were calculated in both coronal and sagittal views for each of the muscles (see Lautenschlager 2013).

Volumetric values for each of the eight muscles were taken from the Avizo 'Material Statistics' function. Physiological cross-sectional area (PCSA) was calculated for each of the muscles, using Equation 1 (Thomason 1991; Taylor *et al.* 2017):

$$\text{PCSA} = \text{volume of muscle}/\text{mean length of muscles fibres} \quad (1)$$

Two separate data sets were then generated for the calculation of absolute muscle force using the intrinsic muscle

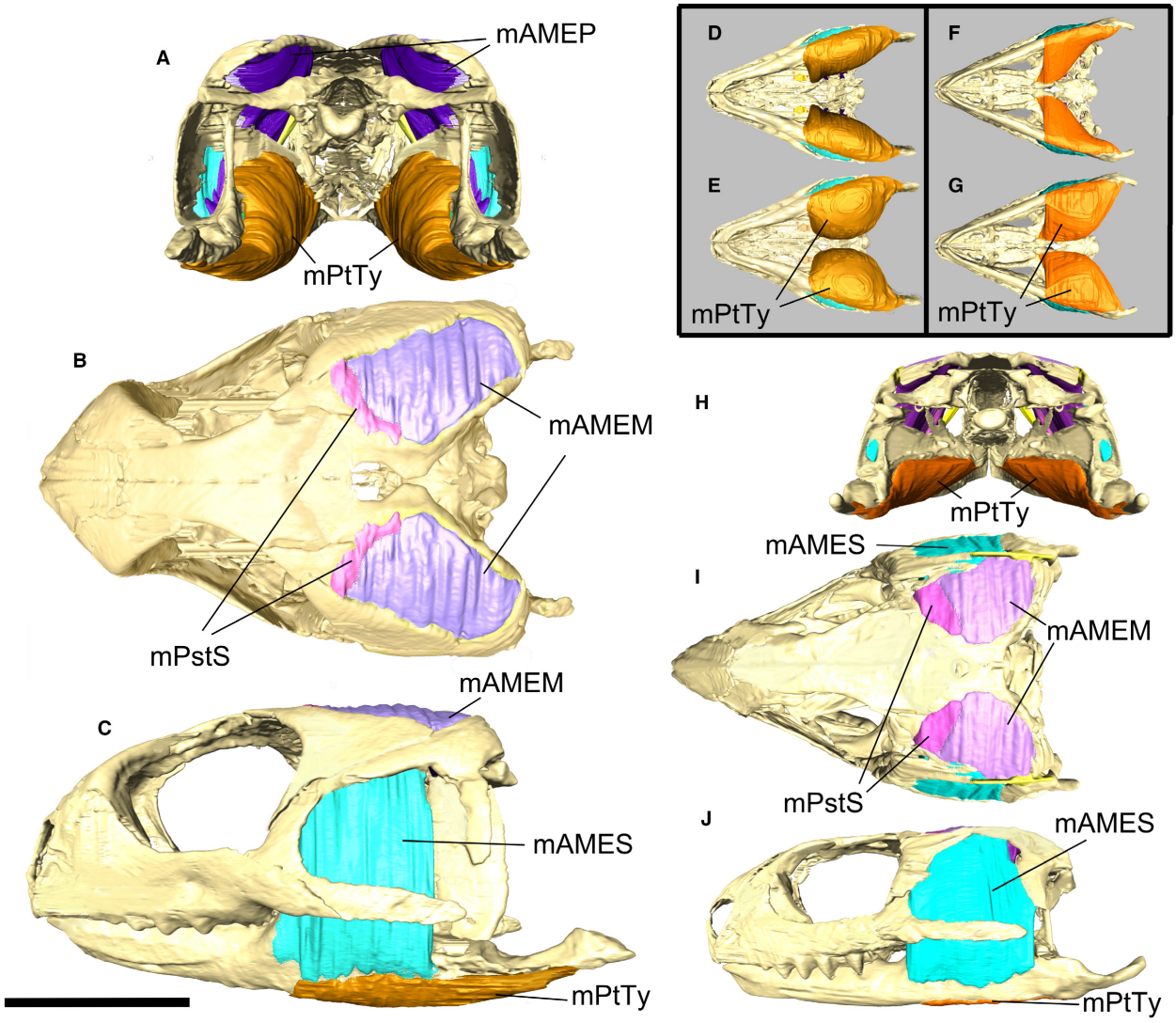

FIG. 4. Adductor muscle reconstruction. A–C, *Clevosaurus hudsoni*X (NHMUK PV R36832) in: A, posterior; B, dorsal; C, lateral view. D–G, two alternative reconstructions for the pterygoideus typicus (mPtTy) in ventral view: D–E, *C. hudsoni*X; F–G, *C. cambrica*. H–J, *C. cambrica* (NHMUK PV R37014) in: H, posterior; I, dorsal; J, lateral view. Scale bar represents 10 mm. Colour online.

values, or muscle stress, (σ) of 0.3 and 0.4 Nmm^{-2} respectively as these values, as well as muscle fibre length, have been found to be the greatest controlling factors in accurate calculations of bite force (Gröning *et al.* 2013). Absolute muscle force (F_{mus}) was calculated using Equation 2:

$$F_{mus} = PCSA \times \sigma \quad (2)$$

Both data sets were then duplicated, resulting in four datasets of absolute muscle force for *C. hudsoni*X, with one of each of the sets being increased by a pennation correction factor of 1.5× (Thomason 1991; Lautenschlager 2013) and the other by a standard muscle force correction factor of 2.75× (Curtis *et al.* 2010). These correction factors were added as bite force is routinely underestimated in lepidosaurs when no such corrections are applied (Curtis *et al.* 2010). Angles of muscle insertion were then accounted for by calculating resulting force vectors using Equation 3 (Lautenschlager 2013), where F_{res} is the resultant muscle force:

$$F_{res} = CosA \times CosB \times F_{mus} \quad (3)$$

Bite forces (F_{bite}) were then calculated at each of the additional dentary teeth for both taxa, four for *C. hudsoni*, and six for *C. cambrica*, using the respective moment arm distances between the muscles and fulcrum (L_{in}), and the distance of the given tooth from the fulcrum (L_{out}). Additional teeth are present in all sphenodontians and are defined as teeth that are added at the posterior of either the dentary or maxilla (Robinson

1976), they are essentially the adult teeth of the animal and are not replaced.

$$F_{bite} = \text{sum}(F_{res} \times L_{in})/L_{out} \quad (4)$$

Also, for direct comparative purposes, the skull and adductor musculature of *C. cambrica* was scaled so that its skull length matched that of *C. hudsoni*X with a muscle volume scaling factor of $(24/19)^3 = 2.015454$.

Mechanical advantage was then calculated at the bite point for each of the dentary teeth.

$$\text{Mechanical advantage (MA)} = F_{bite}/F_{res} = L_{in}/L_{out} \quad (5)$$

Morphology of teeth and tooth pressure

For each of the two species of *Clevosaurus*, ten cross-sectional images down the ultimate dentary tooth, from 10% below the crown to the base of the tooth, were taken from Chambi-Trowell *et al.* (2019; used in Chambi-Trowell *et al.* 2020, fig. S8, but raw data were not published). Maximum and minimum tooth pressures were calculated for each of the taxa down the height of the tooth, using the maximum and minimum biting force obtained for the ultimate tooth, and applying this force over the area of the successive cross-sections of the tooth, following the methods of Gignac & Erickson (2015). The same protocol was followed with *Sphenodon*, with maximum bite force for the ultimate dentary tooth taken as that measured for the female *Sphenodon* used by Jones & Lappin (2009), as its skull length was closest to that of the DigiMorph model.

Beam theory properties of the mandibular rami

Beam theory was applied to the mandibular rami of *Clevosaurus hudsoni*X, *C. cambrica* and *Sphenodon* to assess how their resistance to dorso-ventral and medio-lateral bending and torsion differed between the taxa. Each mandibular ramus was imported into Avizo as a surface .stl file and converted into a solid volume. Using the iso-slice tool, two sets of data were obtained: (1) cross-sectional geometry at 11 equally spaced points from the anteriormost additional tooth to the coronoid process; and (2) cross-sectional geometry at 12 specific homologous points along the entire mandibular ramus (for details on the homologous points, see Chambi-Trowell *et al.* 2020, B). Much of the internally preserved space of the *C. cambrica* mandibular ramus was visible in cross-section, as was that of *Sphenodon*. However, the resolution of the CT scan of *C. hudsoni*X revealed almost no internal morphology. For this reason, all internal spaces for the cross-sectional images of both *Sphenodon* and *C. cambrica* were digitally infilled to account for this difference. The cross-sectional images were then imported into ImageJ, converted into 8-bit TIFF files. Using the plugin MomentMacro (MomentMacroJ v1.4B), section modulus (Z_x, Z_y) and polar moment of inertia (J) were calculated for each of the images. ImageJ was scaled to the appropriate pixels to mm ratio for each specimen. A second data set was then made to recalibrate the other data sets to match the pixels to mm ratio of *C. hudsoni*X, to account for differences in size (e.g. Cuff & Rayfield 2013).

Finite element analysis of the mandibular ramus of Clevosaurus

The repaired right mandibular rami of *Clevosaurus hudsoni*X and *C. cambrica* were imported into Avizo to separate the bones into four components to be analysed: the dentary, articular complex, coronoid and teeth. The angular and articular complex were treated as a single element, as the angular could not be segmented separately within the scans due to lack of resolution of the complete sutural contact. Teeth in *Clevosaurus* are fused to the mandible, and therefore their limits within the mandible are hard to distinguish in the CT scans, so tooth sizes and limits had to be estimated using microphotographs in the literature for both taxa (Keeble *et al.* 2018, fig. 5; Chambi-Trowell *et al.* 2019, fig. 3). The mandibular rami were then exported to Hypermesh (Altair Engineering) for FEA preprocessing and were converted into three-dimensional finite-element meshes comprising linear four-noded tetrahedral (C3D4) elements, with 344 538 elements for *C. hudsoni*X and 281 518 elements for *C. cambrica*. The mesh for *C. cambrica* was then scaled so that the ratio of muscle force to surface area equalled that of *C. hudsoni*X, so that then the models could be compared without size as a factor (see Dumont *et al.* 2009). However, a model with no scaling was also tested (Chambi-Trowell *et al.* 2020, figs S1–S3, tables S3–S4).

The bones of the two mandibular rami were assigned an isotropic and homogenous Young's modulus of 17 GPa and a Poisson's ratio of 0.3, as used previously for *Sphenodon punctatus* (Curtis *et al.* 2011), the only living species of sphenodontian. The teeth were given a Young's modulus of 60.4 GPa and a Poisson's ratio of 0.31, values taken from crocodiles (Creech 2004). Because it is hard to visualize the limits of the muscle attachment sites in such small skulls, particularly between closely positioned muscles, the adductor muscles were assigned to four groups: mAMES, (mAMEP, mAMEM, mPstS, mPstP), mAMP and m. pteryoigdeus (mPtAt, mPtTy), based on natural muscle groups that share similar angles of the line of action. Muscles were added as vectors relative to the

position of the mandibular ramus, and contractile forces for each muscle group were divided among 400 nodes each, with the exception of the mAMP for which 200 nodes were used, following the methods of Taylor *et al.* (2017). The muscle forces used were taken from the mid-range of the calculated values. Twenty-one neighbouring nodes were constrained on the articular condyle. Two models were made for each taxon, one model with 21 nodes constrained at the bite point of the ultimate tooth, and the other model with the same constraint at the bite point of the anteriormost tooth, where all boundary constraints were in all six degrees of freedom, with three in rotational and three in translational. The models were then exported as a solver deck and imported into Abaqus (Dassault Systèmes Simulia, Providence, RI, USA) for processing.

Statistical analyses for beam study on the mandibular ramus

Statistical analyses were conducted for tooth pressure, J, Z_x and Z_y values for the mandibular rami, using SPSS Statistics 24 (IBM Corp., Armonk, NY, USA). Each list of values was assessed independently for normality, using the Shapiro–Wilk test, which is better suited to smaller samples than tests such as Kolmogorov–Smirnov. When all data in a set were non-normally distributed, a non-parametric Wilcoxon ranks test was used to identify significant differences between the three size-scaled taxa for beam values, and absolute values for tooth pressure.

Morphometric analyses of the dentary of rhynchocephalians

We investigated the morphospace occupation for all known rhynchocephalian taxa where a complete, near-complete or full reconstruction of a dentary was available, to compare morphologies between clades, and with a particular focus on clevosaurs. The mandible is primarily adapted for biting (Tseng *et al.* 2011; Gill *et al.* 2014), and it has been found that mandible shape can discriminate between major eco-morphological groups (Kammerer *et al.* 2006; Anderson *et al.* 2011, 2013; Stubbs *et al.* 2013; Herrera-Flores *et al.* 2017). The dentary makes up more than 80% of the mandible and is often the most common well-preserved element in fossil rhynchocephalians (Herrera-Flores *et al.* 2017). It is especially interesting to compare dentaries among species of *Clevosaurus* to determine whether they show any morphological variation linked to proposed feeding ecology, geographic and/or temporal position (Jones *et al.* 2013; Hsiou *et al.* 2015).

The morphometric analysis was performed primarily using the landmark data provided by Herrera-Flores *et al.* (2017), which included 31 taxa, to which we added 8 further taxa (Chambi-Trowell *et al.* 2020, C): *Clevosaurus cambrica* (NHMUK PV R37014; Chambi-Trowell *et al.* 2019), *C.* sp. (AUP 11374; Fraser 1988); *C. hudsoni*X (NHMUK PV R36832; O'Brien *et al.* 2018; Chambi-Trowell *et al.* 2019); *C. wangi*, *C. mcgilli*, *C. petilus* (Wu 1994; Jones 2006); two specimens of *C. bairdi* (NSM 988GF1.1 and reconstruction based on NSM 988GF1.1 + MCZ 9105; Sues *et al.* 1994); and SAM K7890 (a species of *Clevosaurus* from South Africa; Sues & Reisz 1995). We added 13 specimens for species of *Clevosaurus*, where available, for the clevosaur-only morphometric analysis, including the dentaries of two juvenile *Clevosaurus hudsoni* (AUP 11371, Fraser 1988; NHMUK PV R37271, Chambi-Trowell *et al.* 2019, fig. 3E), two sub-adult *Clevosaurus hudsoni* (AUP 11373, Fraser 1988; NHMUK PV R37270, Chambi-Trowell *et al.* 2019, fig. 3D), three additional specimens of adult *Clevosaurus hudsoni* (NHMUK PV R37272, Chambi-Trowell *et al.* 2019, fig. 3F; UMZC T1276, Fraser & Walkden 1983; AUP 11085, Fraser 1988), an additional specimen of *C. cambrica* (Keeble *et al.* 2018, fig. 5C) one juvenile of *Clevosaurus brasiliensis* (UFRGS-PV-0613-T; Romo de Vivar Martinez & Bento Soares 2015), and five additional adult *Clevosaurus brasiliensis* (MCN-PV-2852, UFRGS-PV-0738-T, UFRGS-PV-0606-T, UFRGS-PV-0758-T, UFRGS-PV-0750-T; Romo de Vivar Martinez & Bento Soares 2015); all images were taken from the literature. As for Herrera-Flores *et al.* (2017), all images were of the right dentary, and where not available, a flipped image of the left dentary. We use the same 7 landmarks and 26 semi-landmarks as Herrera-Flores *et al.* 2017, which we coded for our new specimens using the program tpsDig232 (Rohlf 2006) after an image stack .tps had been compiled using tpsUtil32 (Rohlf 2006). A relative warp analysis was then run using tpsrelw32 (Rohlf 2006) to correct for variation in orientation and size of mandibles and images. The data were then imported into R (R Core Team 2019) and a Procrustes superposition analysis was applied to generate a 3D array and a principal component analysis (PCA) carried out, using the package geomorph (Adams & Otárola-Castillo 2013).

Plots were produced using the coordinate data in SPSS (IBM SPSS Statistics 24, 2019) for three subsets of the data:

1. All taxa (one dentary per taxa, adult specimens only).
2. Clevosaurs (all dentaries available for clevosaurs, adult specimens only).
3. Clevosaurs (all dentaries available for clevosaurs, including juveniles).

In the case of *Clevosaurus*, where multiple dentaries were available, we chose type specimens, excluding *Clevosaurus hudsoni* which was represented by the reconstruction by Fraser (1988) and *C. hudsoni*X (NHMUK PV

R36832), the specimen used for this paper. *Sigmala sigmala* is depicted here as a clevosaur because its dentary is similar to that of *C. convallis*, including the dentition and a steep coronoid process typical of all clevosaurs (Säilä 2005; Jones 2006), and following preliminary phylogenetic analyses (unpublished).

The defined groupings for subset 1 are: (1) non-eusphenodontian rhynchocephalians; (2) eusphenodontian rhynchocephalians (excluding clevosaurs); and (3) clevosaurs. For subsets 2 and 3, the groupings are determined by continent (Africa, Asia, Europe, North America, South America) and life stage (adult or juvenile-subadult). These three analyses generated morphospaces for all Rhynchocephalia and for clevosaurs alone.

Groupings of coordinate data for the PCA analysis were tested for statistically significant differences in overlap of morphospace occupancy for subsets 1 and 2. In the subset 2 geographic plot we excluded Africa and North America from the NPMANOVA test as there were only one and two specimens respectively for these two continents. These tests were performed with a one-way NPMANOVA test in PAST (Hammer *et al.* 2001) using Euclidean distances, 10 000 permutations and Bonferroni-corrected p-values; the same parameters used by Herrera-Flores *et al.* (2017).

In addition, we also ran one of the same NPMANOVA tests as Herrera-Flores *et al.* (2017), in which taxa were grouped by geological period (Triassic, Jurassic and Cretaceous).

RESULTS

Bite force, mechanical advantage and tooth properties

Maximum bite force of *Clevosaurus cambrica* is roughly half that of *C. hudsoni*X (Tables 1, 2) at between 50.4% and 52.3% for any matching set (i.e. same values for muscle stress values and correction values). However, when *C. cambrica* was scaled up to match the skull length of *C. hudsoni*X bite force is similar (6.5–18.1N compared to 6.1–19.7N respectively). The mechanical advantage (Table 3) for *C. cambrica* is very similar to that of *C. hudsoni*X posteriorly but diverges anteriorly, which can be partially explained by the fact that *C. cambrica* has more anteriorly positioned anteriormost teeth in the mandible. For a description of the adductor musculature of *Clevosaurus*, see Chambi-Trowell *et al.* (2020, D).

The teeth of *Sphenodon* are near-conical (Fig. 5A), while in *C. hudsoni*X (Fig. 5B) they are mesio-distally elongated and blade-like, and in *C. cambrica* (Fig. 5C) the teeth are also mesio-distally elongated but more complex, with a 'saddle-shape' in which the highest point of the crown is positioned posteriorly with large anterolingually positioned escape structures (Chambi-Trowell *et al.* 2019). Tooth pressure values therefore fall most rapidly at the tip of crown for all three taxa (Fig. 5D; Table 4). How rapidly tooth pressure values decrease depends on the structure of the tooth and therefore cross-section of the tooth (Fig. 5E), for example, the tooth pressure values for *C. cambrica* fall most rapidly out of all three taxa as the tooth area of the crown of *C. cambrica* is much smaller than the cross-sectional area further down the tooth. The values for *C. hudsoni*X fall the most gradually, showing that relatively it maintains a greater tooth pressure for a greater length of its tooth. A Shapiro–Wilk test found the tooth pressure values were not distributed normally ($p = 0.001$), and they were significantly different between species by a Wilcoxon Signed Rank Test ($p = 0.005$).

Mandibular resistance to torsion

Raw values for the polar moment of inertia for the three taxa (Figs 6B, D; 7B, D) differed greatly mainly because of differences in absolute size of the specimens. For example, the mandible of *C. cambrica* (NHMUK R37014) is approximately ~79% the length of *C. hudsoni*X, whereas that of *Sphenodon* (Maisano 2001) is ~240% longer. Because of this, we adjusted values for size by making the measurement of pixels per mm equal for all three taxa. With the values for the full length of the mandible, in the latero-medial direction (Z_x) the two largest peaks in strength in bending (Fig. 7C, D) are seen across the coronoid process and the ultimate tooth, while in the dorsoventral (Z_y) direction the two greatest peaks are across the coronoid process and the articular condyle (Fig. 7E). The values for *Sphenodon* are always greater than those of *Clevosaurus*, suggesting that its jaw is more robust, when

TABLE 1. Bite force calculations for *Clevosaurus hudsoni*X (NHMUK PV R36832).

Tooth	Pennation correction factor × 1.5		Standard muscle force correction factor × 2.75	
	MS = 0.3	MS = 0.4	MS = 0.3	MS = 0.4
1	6.1–8.1	8.1–10.8	11.2–14.8	14.9–19.7
2	5.3–7.0	7.1–9.3	9.7–12.8	12.9–17.1
3	4.7–6.2	6.3–8.3	8.6–11.4	11.5–15.2
4	4.3–5.7	5.8–7.6	7.9–10.5	10.6–14.0
Anterior	3.6–4.7	4.8–6.3	6.5–8.7	8.7–11.5

Maximum bite force ranges (in N) for *Clevosaurus hudsoni*X (NHMUK PV R36832), calculated with differing correction factors and muscle stress values. MS, muscle stress (Nmm^{-2}). The minimum and maximum ranges for each of the rows in the column is the result of two reconstructions of the mPtTy. 'Anterior' indicates the bite force at the mandibular symphysis.

TABLE 2. Bite force calculations for *Clevosaurus cambrica* (NHMUK PV R37014).

Tooth	Pennation correction factor 1.5		Standard muscle force correction factor 2.75	
	MS = 0.3	MS = 0.4	MS = 0.3	MS = 0.4
1	3.1–4.2	4.1–5.6	5.6–7.7	7.5–10.3
2	2.7–3.7	3.6–4.9	4.9–6.8	6.6–9.0
3	2.4–3.2	3.2–4.3	4.3–6.0	5.8–7.9
4	2.1–2.9	2.9–3.9	3.9–5.4	5.2–7.2
5	2.0–2.7	2.6–3.6	3.6–4.9	4.8–6.6
6	1.8–2.5	2.4–3.5	3.4–4.6	4.5–6.1
Anterior	1.5–2.1	2.0–2.8	2.8–3.8	3.7–5.1

Maximum bite force ranges (in N) for *Clevosaurus cambrica* (NHMUK PV R37014), calculated with differing correction factors and muscle stress values. MS, muscle stress (Nmm^{-2}). The minimum and maximum ranges for each of the rows in the column is the result of two reconstructions of the mPtTy. 'Anterior' indicates the bite force at the mandibular symphysis.

TABLE 3. Mechanical advantage of *Clevosaurus hudsoni*X (NHMUK PV R36832).

Tooth	*Clevosaurus hudsoni*X		*Clevosaurus cambrica*	
	Small mPtTy	Large mPtTy	Small mPtTy	Large mPtTy
1	0.43	0.46	0.46	0.42
2	0.38	0.40	0.40	0.37
3	0.33	0.35	0.35	0.33
4	0.31	0.32	0.32	0.30
Anterior/ 5	0.25	0.27	0.29	0.27
6	–	–	0.27	0.25
Anterior	–	–	0.23	0.21

The mechanical advantage measured at the consecutive dentary teeth for *C. hudsoni*X (NHMUK PV R36832) and *C. cambrica* (NHMUK PV R37014), where '–' indicates this tooth is not present in the given taxa. *Clevosaurus hudsoni*X is a proposed second example of Swinton's *C. hudsoni* morphotype (1939). 'Anterior' indicates the bite force at the mandibular symphysis.

adjusted for size. When the measurements forward of the coronoid process (Fig. 6) were analysed, the section modulus (Z_x, Z_y) differs significantly ($p = 0.003$) when taken as a raw value, but when adjusted for size, the difference between *C. hudsoni*X and *C. cambrica* became non-significant ($p = 0.790$ for Z_x, and $p = 0.062$ for Z_y). The polar moments of inertia are all significantly different ($p = 0.003$) when taken as raw values, but when adjusted for size, the difference between *C. hudsoni*X and *C. cambrica* becomes non-significant ($p = 0.929$). Therefore, when adjusted for size, there are no significant differences between the two *Clevosaurus* species.

Finite element analysis of the mandibular rami

Non-directional von Mises stress and maximum principal strain values were recorded for models simulating biting at the ultimate and anteriormost tooth for both taxa (see Chambi-Trowell *et al.* 2020, tables S3–S5, figs S1–S5). In both biting scenarios, maximum overall stresses were observed both directly in front of and behind the coronoid process (Fig. 8A–B, E–F; Table 5; Chambi-Trowell *et al.* 2020, figs S2, S4). The greatest region of stress is positioned posteriorly in *C. cambrica* in the region immediately anterior to the articular condyle, whereas in *C. hudsoni*X it is directly in front of the coronoid process. An anterior bite results in an overall greater distribution of stress encountered by the entire mandibular ramus for both taxa (Fig. 8C–D, G–H), and von Mises stress values (median) were overall higher for *C. cambrica* than *C. hudsoni*X (Table 5). Maximum von Mises stress values for *C. hudsoni*X range between ~86 and 106 MPa, while for *C. cambrica* the values are 127–171 MPa, which suggests a high risk of failure in the mandibular ramus (Currey 2002). However, it should also be noted that because of the way in which the jaw was scaled, the surface area was disproportionally smaller compared to the muscle force that would have been active in the unscaled model, and values for the unscaled model fall within more natural limits (Chambi-Trowell *et al.* 2020, tables S3, S4). Overall, this suggests that the mandibular ramus of *C. cambrica* had a lower strength–stress performance than that of *C. hudsoni*X. In addition, strain values were overall greater for *C. cambrica* than *C. hudsoni*X. In both specimens, stresses decrease anteriorly up the coronoid process, before increasing immediately in front of it.

Morphometric analysis

The NPMANOVA test on the results from the morphometric analysis (Fig. 9A) shows that all three groups (clevosaurs, 'basal taxa', and sphenodontians excluding clevosaurs) are significantly different (Table 6).

The continent-scale comparisons of clevosaurs (Fig. 9B) shows that all groups were significantly different with the exception of Asian and European clevosaurs (Table 7). When juveniles are included (Fig. 9C), the clevosaurs from each continent show differences in form, which might relate to the geographical distances separating them and presumed absence of interbreeding. The taxon that is closest to the average shape is *C. sectumsemper*; followed by *Palaeopleurosaurus*, *Pamizinsaurus* and *Clevosaurus cambrica*. Note that *Pamizinsaurus* is represented by a juvenile (with no other known specimens; Reynoso 1997) and may not reflect the morphology of an

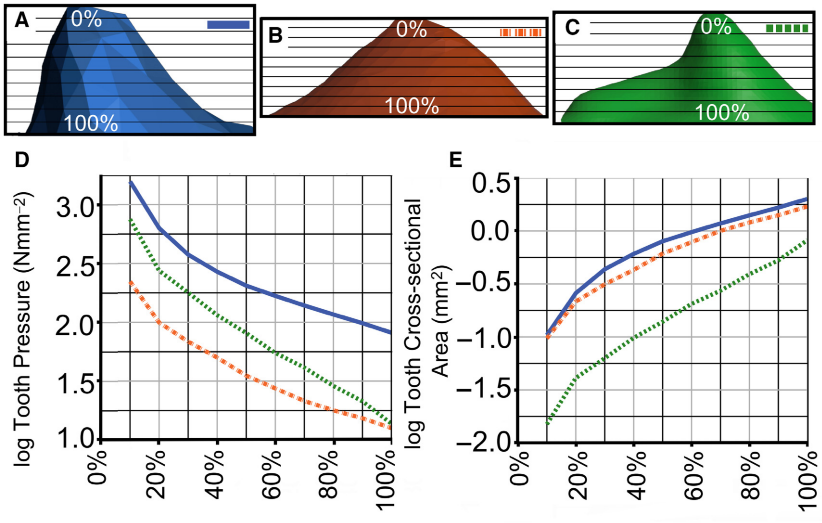

FIG. 5. Log biomechanical values for the right ultimate dentary tooth (in lateral) for: A, *Sphenodon* (Maisano 2001); B, *Clevosaurus hudsoni*X (NHMUK PV R36832); C, *C. cambrica* (NHMUK PV R37014). D, tooth pressure. E, cross-sectional area. Colour online.

TABLE 4. Mechanical advantage of *Clevosaurus hudsoni*X (NHMUK PV R37014).

Relative distance from crown	*Clevosaurus cambrica*	*Clevosaurus hudsoni*X
10%	205.0–688.1	62.9–203.3
20%	75.0–251.7	28.2–91.3
30%	48.8–163.8	19.4–62.8
40%	31.4–105.3	14.2–46.0
50%	22.1–74.3	10.0–32.3
60%	15.0–50.3	7.8–25.2
70%	11.3–37.8	6.1–19.7
80%	7.9–26.4	5.1–16.4
90%	5.8–19.5	4.3–14.0
100%	3.8–12.6	3.6–11.6

Calculated potential tooth pressure range (MPa) for the ultimate dentary tooth of *C. hudsoni*X (NHMUK PV R36832) and *C. cambrica* (NHMUK PV R37014), measured from the crown downwards. *Clevosaurus hudsoni*X is a proposed second example of Swinton's *C. hudsoni* morphotype (1939).

adult. The three that are furthest in morphospace from the common shape, starting with least similar, are *Pleurosaurus*, *Clevosaurus bairdii* and *Clevosaurus brasiliensis*.

The NPMANOVA test for taxa grouped by geological period (Fig. 9D; Table 8) shows results that are congruent with those of Herrera-Flores *et al.* (2017). We confirm that Triassic rhynchocephalians are significantly different from Cretaceous rhynchocephalians ($p = 0.0321$), while Cretaceous and Jurassic rhynchocephalians are not significantly different in their morphology. We also find that Triassic rhynchocephalians are significantly different in their morphology from Jurassic rhynchocephalians ($p = 0.0192$), suggesting a transition in morphology across the Triassic–Jurassic boundary.

DISCUSSION

The bite force of Clevosaurus

Maximum bite force is a key factor in defining dietary niches, as food hardness can define the dietary scope (Verwaijen *et al.* 2002; Aguirre *et al.* 2003) and affect dietary interspecific competition (Cornette *et al.* 2015). The teeth of *Clevosaurus* are relatively large and reduced in number compared to more basal rhynchocephalians. These stouter, larger teeth would have been resistant to loading and torsional forces (Fraser 1988; Jones 2009). The jaws are further reinforced with a secondary growth of bone that extends from the teeth and partially envelops the maxilla and dentary bones, forming a longitudinal lip of secondary bone. With the extreme wear facets visible on the teeth of all *Clevosaurus*, they probably had comparatively high bite forces compared to their predecessors, a view that is supported by a relatively expanded postorbital region, allowing for a greater volume of adductor musculature, and somewhat short, robust skulls that would have been resistant to bending and torsion (Jones 2008, 2009). A high initial bite force is vital to incapacitate prey and to provide high enough forces to create stress points to allow the teeth to penetrate the prey item in food reduction (Gorniak *et al.* 1982; Verwaijen *et al.* 2002).

The maximum estimated bite force (~6.1–19.7N) for *C. hudsoni*X (*C. hudsoni* was ~250 mm, with an estimated snout-to-vent length (svl) of 145 mm; Fraser 1988) is roughly comparable to that of a neonate Alligator with a bite force of 9.4–12.1 N and an svl of 131–143 mm (Erickson *et al.* 2003; Gignac & Erickson 2015). This is higher than the 8.7 (±3.1) N range suggested for

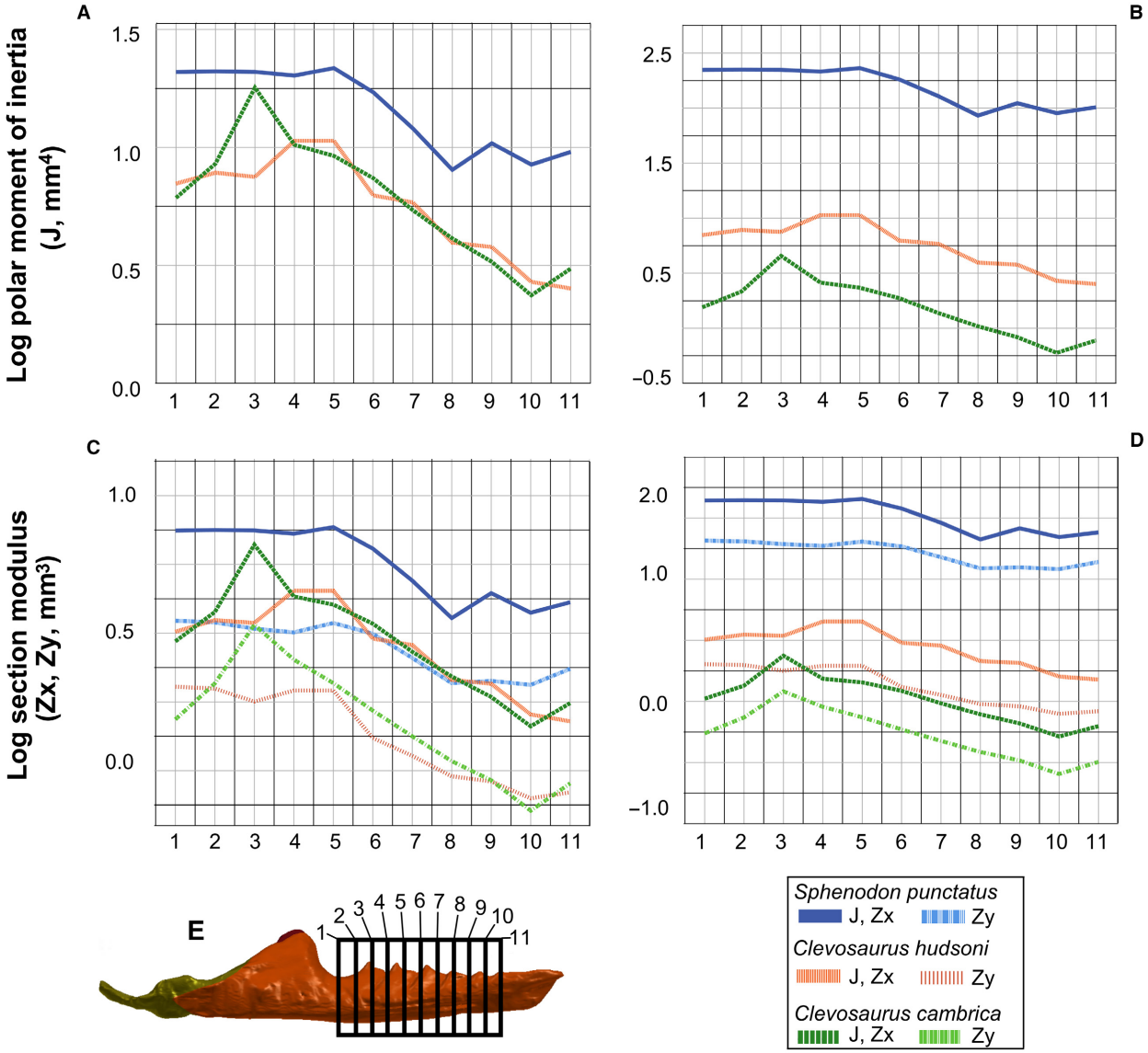

FIG. 6. Logged beam theory analysis output for the cross-sectional regions for the anteriormost portion of the dentary for *Clevosaurus hudsoni*X (NHMUK PV R36832), *Clevosaurus cambrica* (NHMUK PV R37014) and *Sphenodon* (Maisano 2001), taken at equal distances between the anteriormost additional tooth to the coronoid process. A, C, polar moment of inertia (mm^4); B, D, sectional modulus (mm^3); A, C, dentaries are scaled to the same size; B, D, raw data. E, cross-sectional sites indicated on the mandible of *Clevosaurus cambrica*. Colour online.

a juvenile *Sphenodon* with cranial length of 20–25 mm and an svl of 96 mm (±9.1 mm) in Schaerlaeken *et al.* (2008), and similar to the ~11–12 N range suggested for agamid lizards with the same cranial length in the same study. Note that ontogenetic change in the morphology of the skull of *Sphenodon* must not be forgotten, as the adductor chambers of a juvenile *Sphenodon* are relatively much smaller than those of an adult (Schaerlaeken *et al.* 2008).

While bite forces for *Sphenodon* with skull lengths of 19 mm (as *C. cambrica*; NHMUK PV R37014) were not measured (Schaerlaeken *et al.* 2008), interpolation, and assuming isometric scaling, suggests a magnitude of around 3–5 N, while the bite force of 11 N for agamid lizards surpasses the maximum estimated bite force range for *C. cambrica* (~3.1–10.3 N). Small lacertid lizards with cranial lengths of 14.9–15.1 mm were found to produce bite forces of 5.9–6.7 N (Verwaijen *et al.* 2002), which falls within both estimated ranges for *C. cambrica*. However, these animals have skulls that are ~21% shorter than *C. cambrica*, which suggests that the latter could generate bite forces towards the upper end of the range and similar to an equivalently sized agamid. When scaled so that the cranial length of *C. cambrica* matched that of

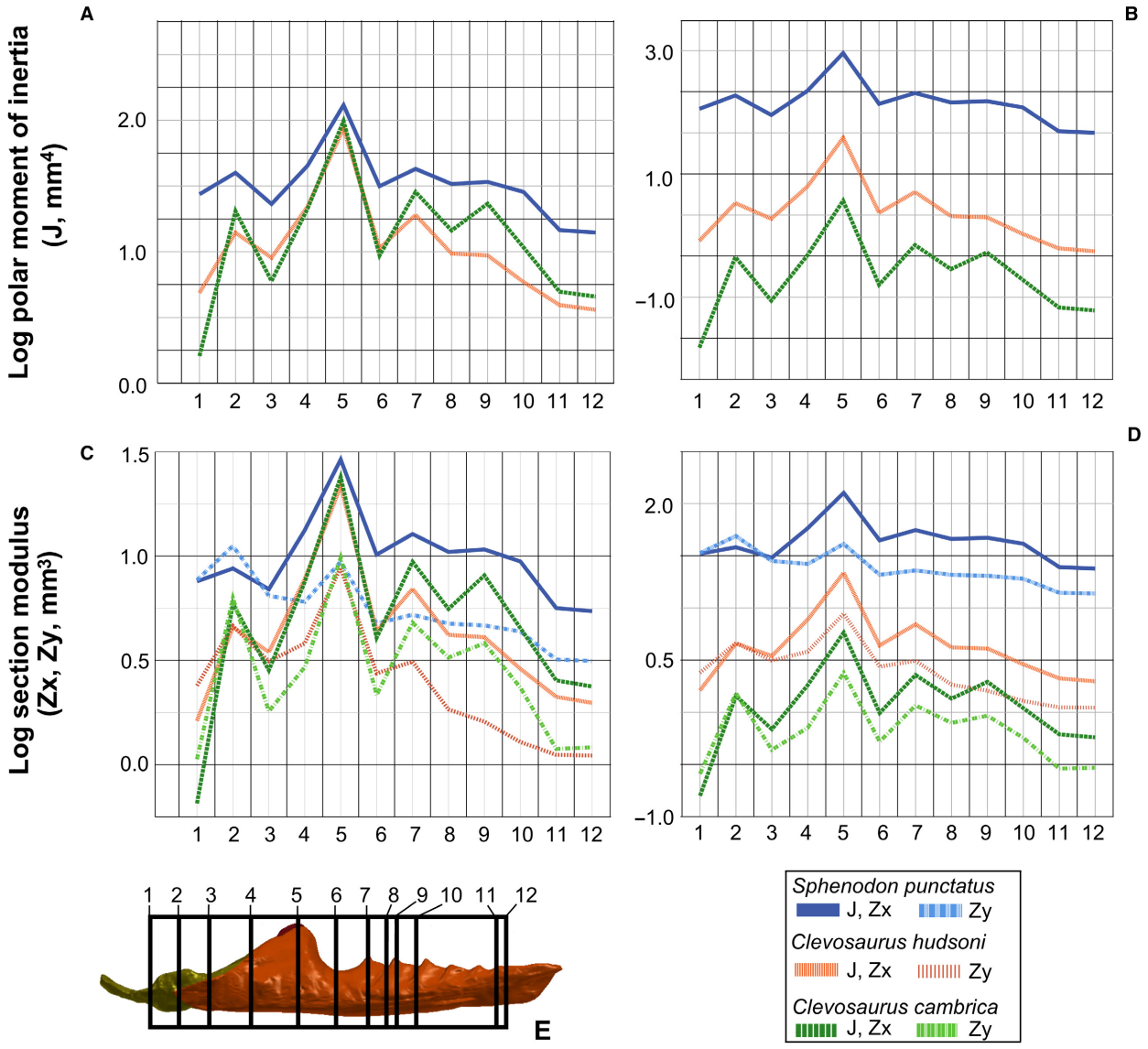

FIG. 7. Logged beam theory analysis output for the cross-sectional regions for the mandibular ramus for *Clevosaurus hudsoni*X (NHMUK PV R36832), *Clevosaurus cambrica* (NHMUK PV R37014) and *Sphenodon* (Maisano 2001), taken at specific homologous sites (Chambi-Trowell *et al.* 2020, B). A, C, polar moment of inertia (mm^4); B, D, sectional modulus (mm^3). A, C, dentaries are scaled to be the same size; B, D, raw data. E, cross-sectional sites indicated on the mandible of *Clevosaurus cambrica*. Colour online.

*C. hudsoni*X, they share a very similar bite force range. Therefore, our estimates suggest that clevosaurs had bite forces more in line with modern insectivorous agamid lizards than with *Sphenodon*. However, *Sphenodon* has a horizontal propalinal component of bite force that tears at the food item, unlike *Clevosaurus* where the bite was entirely orthal (Whiteside 1983; Jones 2009) and this perhaps enables the modern taxon to process its food, after piercing, with a lower maximum bite force.

For insectivorous mammaliaforms of similar size, a bite force of 2–3 N was found to be necessary to break apart the chitin of a prey item such as a 10 mm-long beetle (Gill *et al.* 2014). The mandible lengths from condyle to mandibular symphysis were slightly over 17.5 mm and 20.0 mm respectively for *Morganucodon* and *Kuehneotherium*, less than but close to the 19 mm and 24 mm mandibular lengths of *C. cambrica* and *C. hudsoni*X. Both *Clevosaurus* species exceed the bite force requirement for piercing cuticle, even at the lower end of the range of maximum bite force estimates (Tables 1, 2), and therefore appear capable of processing hard cuticle of appropriately sized prey, and perhaps even the harder exoskeletons of terrestrial myriapods, which are known to have been contemporary in Cromhall Quarry (Whiteside *et al.* 2016).

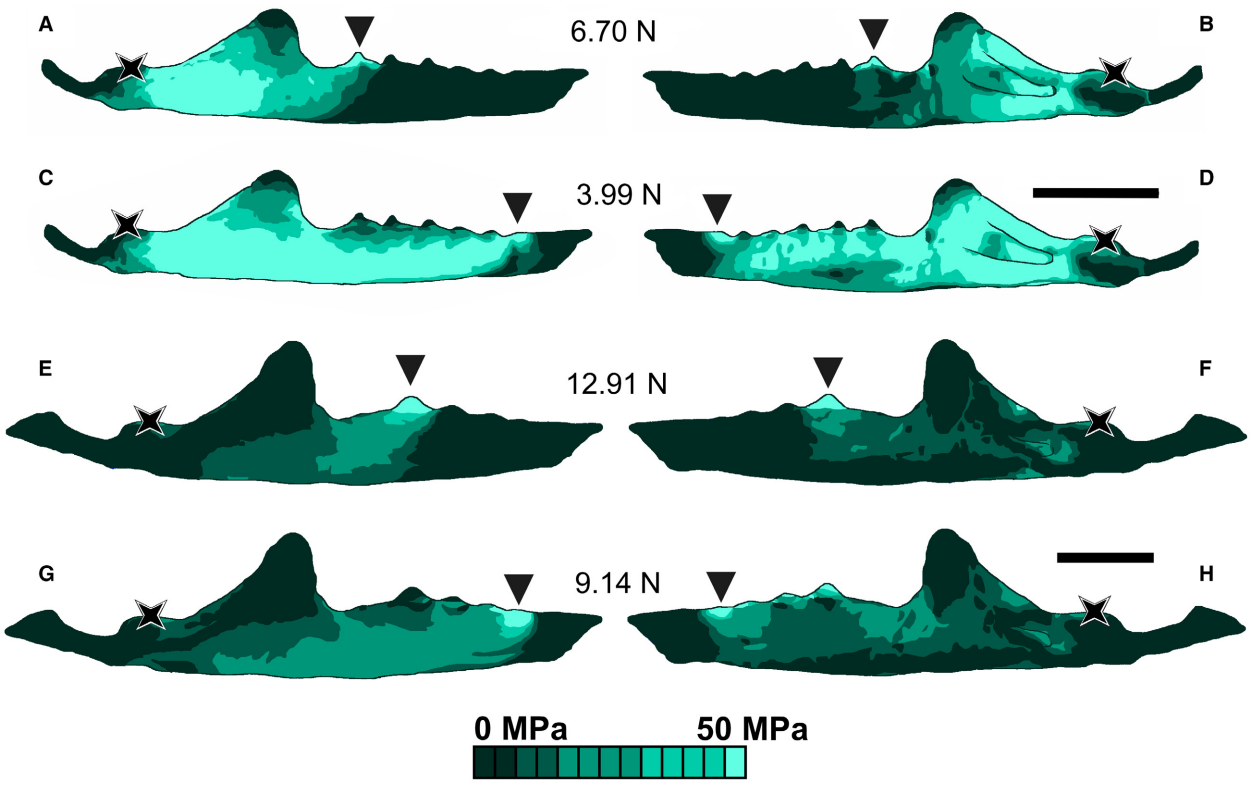

FIG. 8. Finite element von Mises stress contour plots for the right mandibular ramus of *Clevosaurus cambrica* (NHMUK PV R37014) and mandibular ramus of *C. hudsoni*X (NHMUK PV R36832). A–D, *Clevosaurus cambrica*, with a bite point at the ultimate tooth in: A, lateral; B, medial view; and for the anteriormost tooth in: C, lateral; D, medial view. E–H, *Clevosaurus hudsoni*X, for a bite point at the ultimate tooth in: E, lateral; F, medial view; and for the anteriormost tooth in: G, lateral; H, medial view. Bite point is indicated with an arrow; condyle/fulcrum is indicated with a star. Scale bars represent 5 mm. Colour online.

TABLE 5. Finite element analysis output for *Clevosaurus*.

	Clevosaurus cambrica		*Clevosaurus hudsoni*X	
	Ultimate tooth	Anteriormost tooth	Ultimate tooth	Anteriormost tooth
Maximum von Mises stress (MPa)	127.30	171.23	106.09	86.73
Maximum principal strain (microstrain)	4.63×10^{-3}	8.86×10^{-3}	1.21×10^{-3}	1.56×10^{-3}
Maximum bite force values (N)	6.70	3.99	12.91	9.14
Median von Mises stress stress (MPa)	11.72	33.20	4.59	5.71
Median principal strain (microstrain)	4.74×10^{-4}	1.27×10^{-3}	1.91×10^{-4}	2.30×10^{-4}

FEA output for the mandibles of *C. cambrica* (NHMUK PV R37014) and *C. hudsoni*X (NHMUK PV R36832), scaled so that they share the same muscle force to surface area ratio. *Clevosaurus hudsoni*X is a proposed second example of Swinton's *C. hudsoni* morphotype (1939). maximum von Mises stress and maximum principal strain taken as a 0.995 percentile of output.

The prominent palatine tooth row of *Sphenodon* and other sphenodontians provides a unique cutting surface. In *Sphenodon* both the maxillary and palatine teeth hold the food item taut while it is sheared by the dentary teeth, forming a three-point contact with the food item (Gorniak *et al.* 1982). The double tooth rows in rhynchocephalians may have evolved as a functionally equivalent structure to the multicuspid mammalian tooth, but at a cost. Though their blade-like teeth may be analogous to the carnassials of mammals, *Clevosaurus* would have had limited, or no, movement of its mandible about the long axis, not simply because of the need for precise occlusion, but also the row of palatine teeth would limit lateral movement of the mandible during biting (Gorniak *et al.* 1982). In *Morganucodon*, a 20° mesial or anterior deviation from orthal is possible in a single biting stroke (Jäger

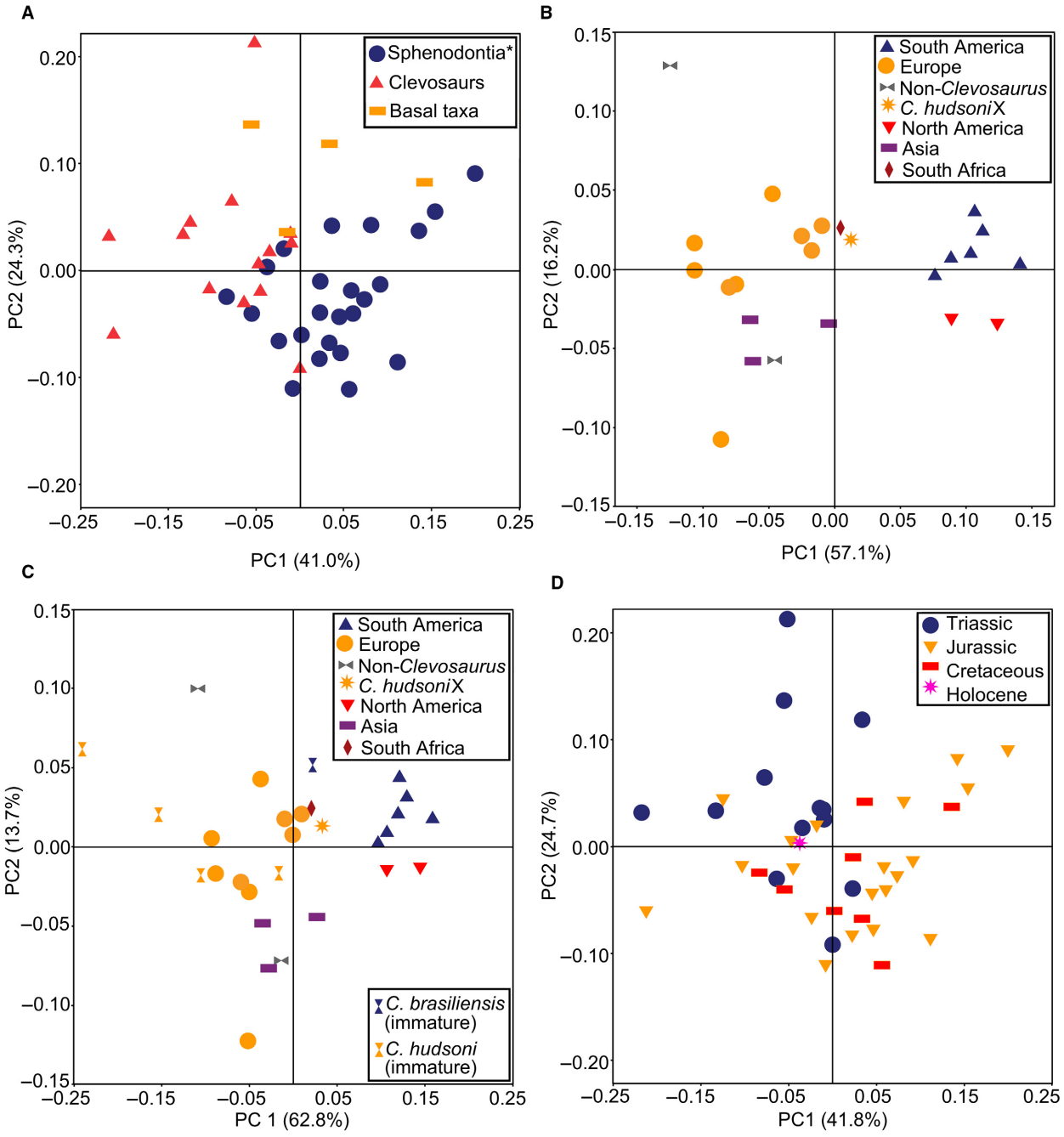

FIG. 9. Dentary morphospace occupation based on a morphometric analysis for Rhynchocephalia and clevosaurs. A, Rhynchocephalia; *Sphenodontians excluding *Planocephalosaurus*. B, clevosaurs grouped by continent. C, clevosaurs group by continent, including juvenile specimens. D, Rhynchocephalia grouped by geological period. Colour online.

et al. 2019), whereas the guiding structures in *Clevosaurus*, the pterygoid flange and palatine teeth, indicate auto-occlusion. This might have placed sphenodontians at an evolutionary disadvantage to mammaliaforms as it would have prevented them from developing any form of transverse mastication, which has proved very successful in mammals (Gorniak *et al.* 1982).

The mechanical advantage of Clevosaurus

Bite force can be calculated directly from digital reconstructions of muscles in fossil taxa, but its efficiency can also be inferred indirectly by measuring mechanical advantage. Mechanical advantage corresponds to the efficiency of a biting mechanism, with high values indicating

TABLE 6. Morphometric analysis output for Rhynchocephalia.

	Clevosaurs	'Basal taxa'	Sphenodontians (exc. clevosaurs)
Clevosaurs	—	0.0195	0.0003
'Basal taxa'	0.0195	—	0.0096
Sphenodontians (exc. clevosaurs)	0.0003	0.0096	—

p-values for the NPMANOVA test for the output of a morphometric analysis for dentary morphospace occupation of Rhynchocephalia, comparing clevosaurs, 'basal taxa' and sphenodontians (excluding clevosaurs).

TABLE 7. Morphometric analysis output for *Clevosaurus*.

	Europe	Asia	South America
Europe	—	0.2674	0.0001
Asia	0.2674	—	0.0137
South America	0.0001	0.0137	—

p-values for the NPMANOVA test for the output of a morphometric analysis for dentary morphospace occupation of Rhynchocephalia, comparing Mesozoic rhynchocephalians by continent.

TABLE 8. Morphometric analysis output for Rhynchocephalia by geological period.

	Triassic	Jurassic	Cretaceous
Triassic	—	0.0192	0.0321
Jurassic	0.0192	—	1
Cretaceous	0.0321	1	—

p-values for the NPMANOVA test for the output of for the output of a morphometric analysis for dentary morphospace occupation of Rhynchocephalia, comparing Mesozoic rhynchocephalians by geological period.

a very efficient transfer of in-force of the adductor musculature into out-force at the given bite point (Gill *et al.* 2014; Cornette *et al.* 2015). The mechanical advantage of the ultimate tooth was similar for both *Clevosaurus* species, with a value of ~0.43–0.46 for *C. hudsoni*X and ~0.42–0.46 for *C. cambrica*. These ranges are less than that of the early mammaliaform *Morganucodon* (0.51; Gill *et al.* 2014) but greater than that of the early mammaliaform *Kuehneotherium* (0.31; Gill *et al.* 2014). As the mechanical advantages for both species of *Clevosaurus* fall in the general range shared by these mammaliaform insectivores, this does not dismiss the possibility of dietary overlap between the two.

The mechanical advantages for the anteriormost teeth of *C. cambrica* are lower than in *C. hudsoni*X, partly because the anteriormost teeth are more mesially placed in the former. *Clevosaurus cambrica* then may have had a quicker but less forceful bite, before manipulation and posterior movement of the prey to the back of the tooth row, where tooth pressures would have been much higher and could have helped to quickly kill and reduce prey items. This posterior shift of large prey items is seen in *Sphenodon* (Gorniak *et al.* 1982). In sphenodontians, teeth are added posteriorly to the tooth row, so they are always larger, less worn and more effective as a shearing surface than earlier emplaced, more anterior teeth.

Clevosaurus cambrica is diagnosed by the fact that its penultimate dentary tooth is the largest, not the ultimate (Keeble *et al.* 2018), unlike most *Clevosaurus* (but cf. *C. convallis*; Säilä 2005). Further, there is a trade-off in terms of prey size in that the more posterior positioning of greatest bite force leaves a smaller gap but a higher mechanical advantage of the adductor muscles (Gorniak *et al.* 1982). Perhaps the unique teeth of *C. cambrica* indicate a more anterior positioning of prey during reduction, albeit with the trade-off of a lower mechanical advantage and bite force but perhaps allowing it to take whole small arthropod prey into its jaws. With a speculated faster but lower bite force than *C. hudsoni*X, *C. cambrica* may have specialized on small faster invertebrate prey, whereas *C. hudsoni*X, with the greater mechanical advantage of its anteriormost tooth, and overall more evenly distributed mechanical advantages of its dentary teeth and greater bite force, could have dealt with slower and harder prey, possibly including beetles, millipedes, scorpions, isopods and small vertebrates.

Tooth pressure in Clevosaurus *and* Sphenodon

Unlike mammaliaforms, sphenodontians characteristically have a double row of maxillary-palatine teeth, which means that the relative tooth pressure was always greatest on the single row of mandibular teeth. This is because of their smaller surface-area of contact with the food item, meaning that the mandibular teeth always penetrate the food item first (see Gorniak *et al.* 1982). This in turn means that the tooth pressure upon the ultimate dentary tooth is roughly twice that of the corresponding maxilla-palatine teeth, and for this reason, a focus on mandibular tooth pressure provides a more reliable value of forces during feeding.

As described by Chambi-Trowell *et al.* (2019), dentary tooth shape differs between the two species. The teeth of *C. cambrica* (NHMUK PV R37014) have a saddle-shaped lateral profile with a large anterolateral flange, with the posterior edge of the cusp being raised and pointed, while anterolingually there is a large escape structure, and the long axes of the teeth are arranged at an angle to the long axes of the mandibular ramus so that they cut like pinking shears. By contrast the dentary teeth of *C. hudsoni*X have a triangular lateral profile, with the highest point of the cusp being central, and they have no or poorly pronounced escape structures, the long axes of the teeth being aligned so that they form a straight continuous cutting surface like a bread knife. It is important to note, however, that the additional dentary teeth of *C. hudsoni* normally share the same saddle-shaped profile of *C. cambrica*. The teeth of *C. cambrica* would have produced more damage than those of *C. hudsoni*X after puncturing the prey item, but this came at the cost of a more rapidly reduced tooth pressure down the height of the tooth, a pattern seen in the molariform teeth of crocodilians (Erickson *et al.* 2012). Chambi-Trowell *et al.* (2019) suggested that the teeth of *C. cambrica* were better suited to breaking chitin apart through expansive damage, while the teeth of *C. hudsoni*X were better suited to slicing.

For both species of *Clevosaurus*, tooth pressure value ranges are high enough to break apart chitin (Table 4; shear strength of chitin is 25–54 MPa, Currey 1967) supporting the idea that they ate arthropods. Chitin is often laid down in parallel layers, which means that long blade-like teeth like those of *Clevosaurus*, are ideal for penetrating the woven structure, at least in insectivorous mammals (Lucas & Peters 2007). Chitin can be oriented in the mouth if, like *Sphenodon*, *Clevosaurus* used a muscular tongue or rapid movements of the head to reposition its prey during reduction (Gorniak *et al.* 1982). With its larger escape structures, *C. cambrica* may have been able to process food more rapidly (Chambi-Trowell *et al.* 2019) than *C. hudsoni*X as the structures would have allowed it to clear food fragments from the main cutting surface more rapidly. This suggests that *C. cambrica* may have taken smaller prey items than *C. hudsoni*X, just as in *Sphenodon* today, which processes larger food items more slowly (Gorniak *et al.* 1982).

Peak resistances to torsion and bending are seen for both *Clevosaurus* species across the ultimate tooth, coronoid process and articular condyle (Fig. 7). For example, the high coronoid process of *C. hudsoni*X resists torsion four times more effectively than at any other point on its mandible, while it is three times in *C. cambrica*. The lower resistances to torsion immediately on either side of the coronoid process found in the FEA of the mandibles of *C. hudsoni*X and *C. cambrica* confirms that these regions are subject to greater stress during biting (Fig. 8). When adjusted for size, *C. cambrica* has relatively higher resistance to torsion and bending in its mandible than *C. hudsoni*X, perhaps corresponding to greater stresses in its gracile mandible during biting (Table 5). The stress values decrease anteriorly from the articular condyle towards the coronoid process, and it is possible that the highest regions of stress below the coronoid process are mitigated in rhynchocephalians by the high coronoid process with its resistance to torsion and bending.

The ultimate shear stress of bone is 65–71 MPa (Carter & Beaupré 2001), and perhaps both species of *Clevosaurus* had tooth pressures great enough to overcome this (Table 4), *C. cambrica* notably more so than *C. hudsoni*X. *Clevosaurus cambrica* could maintain the necessary pressure for up to 20–50% of its tooth height, whereas *C. hudsoni*X might have been able to achieve this only up to a maximum possible height of 20%. However, the resistances to bending and torsion in the teeth of *C. cambrica* are much lower than in *C. hudsoni*X, meaning that *C. cambrica* was more effective at piercing prey, but its teeth were at greater risk of breaking, and this would have affected their prey choice, as is seen also in slender-snouted crocodilians (Erickson *et al.* 2012).

Could species of *Clevosaurus* have attacked vertebrate prey? In a study by Vervust *et al.* (2009), it was found that the bite force required to break phalanges of some small squamates ranges from ~8 to 18 N, which *C. hudsoni*X could have exceeded at the mid to higher range of its estimated bite forces, but which *C. cambrica* (NHMUK PV R37014) would have struggled to exceed only at its highest estimated bite force. However, Vervust *et al.* (2009) noted that bite forces by predators were lower than the toe bone strength of prey during predatory episodes they observed. Bone does not need to be broken for a predator to be able to disassemble a prey item; it merely has to overcome the strength of connective tissue. *Sphenodon* moves its entire head when feeding on large prey (Gorniak *et al.* 1982), and *Clevosaurus* might have done the same by shaking small vertebrates to bits. It should also be noted that *C. cambrica* might have reached the same skull length (~24 mm; Keeble *et al.* 2018) as *C. hudsoni*X, and at that size its bite force would have been equivalent. Therefore, larger specimens of *C. cambrica* might well have been capable of taking small vertebrate prey. This suggestion is supported by the prominent deep wear facets below the posterior teeth of the dentary formed by occlusion with the opposing maxillary teeth, thus demonstrating that both species of *Clevosaurus* had sufficient bite force to cut bone.

These conclusions contrast with the earlier suggestion (Fraser & Walkden 1983; Fraser 1988) that *C. hudsoni* was a herbivore. *Clevosaurus hudsoni* could have used its blade-like teeth for cropping vegetation, although these teeth seem short in comparison to the longer blades of

herbivorous procolophonids and lizards such as *Uromastyx* (Sokol 1967; Moazen *et al.* 2008). It is also worth noting that *Uromastyx* with similarly sized skulls (~24–26 mm) have been recorded with bite forces above the values calculated for *Clevosaurus* here, at ~23–47 N, possibly indicating that herbivorous squamates may require greater bite forces to break down coarse vegetation (Herrel *et al.* 2013). However, these values should be considered with caution as there appears to be sexual dimorphism in bite force in the dataset for *Uromastyx* in Herrel *et al.* 2013, with males displaying bite forces around twice as high as similarly sized females. This requires further investigation using approaches such as tooth microwear analysis and FEA of the skull to compare it to extant herbivorous lizards such as *Uromastyx*, where stresses are focused in the frontals and nasals during mastication (Moazen *et al.* 2008).

Morphometric analyses

With 11 species currently attributed to the genus *Clevosaurus* alone, almost half of which are found in the UK, clevosaurs are one of the most speciose groups of rhynchocephalians and, as revealed here (Fig. 9A), a morphologically disparate group. Three species of *Clevosaurus* from China, though, are debated, with *C. petilus* and *C. wangi* possibly synonymous (Sues *et al.* 1994), while others have concluded that the material is so fragmentary that it would be wise to group all three taxa together as *Clevosaurus* spp. (Jones 2006). If this is the case, then most known *Clevosaurus* diversity is in the UK, but this could reflect biased sampling. On the other hand, the high diversity of *Clevosaurus* in the UK could represent an adaptive radiation on the archipelago of Triassic–Jurassic islands in the Bristol Channel area (Whiteside *et al.* 2016).

In our morphometric analysis, we found that clevosaurs are morphologically distinct from other rhynchocephalians, suggesting that they occupied a specific niche that appears to have closed during the Jurassic, coinciding with the diversification of mammaliaforms and squamates (Milner *et al.* 2000; Evans *et al.* 2001; Apesteguía 2005). The oldest *Clevosaurus*, *C. hadropodon* (Hsiou *et al.* 2019), has been named from the Carnian but the material is insufficient to confirm its identity as a clevosaur (or its affinities with Rhynchocephalia) and it is not included in this analysis. *Clevosaurus brasiliensis* is the oldest certain *Clevosaurus*, and was morphologically distinct from all other species within the genus, while Chinese clevosaurs were the least distinct, being significantly different only from *C. brasiliensis* although, as noted, the distinctiveness of these Chinese taxa requires restudy and these dentaries are based on reconstructions which may have been influenced by the more complete material available for European *Clevosaurus*. We found that the European clevosaurs are distinct from South American but not Chinese clevosaurs. In addition to geography, some variation might also be explained by age. The European clevosaurs are mainly Rhaetian, except *Clevosaurus convallis* (probably earliest Jurassic; Whiteside *et al.* 2016), whose mandible shape is distinct from other UK species, while *Clevosaurus brasiliensis* in South America could possibly be as old as Norian (Bonaparte & Sues 2006). The North American and Chinese clevosaurs are from the Lower Jurassic (Sues *et al.* 1994; Wu 1994).

Limitations of the muscle reconstruction

The reconstruction of muscle attachment points was limited by the extent of preservation and the reconstruction of the skull itself, particularly around the retroarticular process. Some muscles had origin and insertion sites in non-preserved soft-tissue processes, and such sites of attachment had to be estimated in three-dimensional space. In addition, osteological correlates are often very subtle in smaller animals, and the smaller of the two skulls was less than 20 mm long. However, in other recent studies muscles have been reconstructed using similar methods for similarly sized skulls, the smallest of which was 24.9 mm (*Mus musculus*; Adams *et al.* 2019).

Muscle volumes were standardized relative to one another within the cranium through the use of straight connections between the extents of muscle attachment sites. Muscle volumes were increased until the adductor chambers were filled. The shapes of these muscles were simplified, and so individual muscle volumes cannot always be given. Muscle volumes were constrained primarily by the adductor chambers but estimates had to be made for those outside the cranium, namely the pterygoideus typicus.

Reconstruction of the bite force assumes 100% activation of all adductor musculature, which is unlikely, and in *Sphenodon*, as in other vertebrates, different muscles activate at different times during the bite cycle (Gorniak *et al.* 1982). A further difficulty is that *Sphenodon* has a propalinal jaw motion, different from the direct orthal shear of *Clevosaurus*. We also had to simplify muscle fibre length and line of action, both of which impact bite force calculations (Gröning *et al.* 2013) and both vary in *Sphenodon* (Gorniak *et al.* 1982). This was accounted for by taking the mean of multiple measurements. Muscle wrapping was also recreated, albeit simplistically, as this is known to affect the mean fibre length (Gröning *et al.* 2013).

In preparing the FEA model of the mandibular rami, it was assumed that the bones of the jaws were isotropic. This has been shown not to affect the overall distribution of stress values and removes the possibility of

unquantifiable artefacts induced by anisotropy (Strait *et al.* 2005; Moazen *et al.* 2008; Gill *et al.* 2014). Values of bone material properties cannot be tested for extinct taxa, so the values were taken from *Sphenodon*, the closest extant relative of *Clevosaurus*, and crocodilians.

CONCLUSIONS

Here for the first time we evaluate the biomechanical properties of the teeth and jaws of two early sphenodontians, providing the first biomechanical data for *Clevosaurus*. We find that *Clevosaurus* could have competed with early mammaliaforms over dietary resources. Both *Clevosaurus* species investigated had mechanical advantages that fall within the ranges of values calculated for early Mesozoic mammaliaforms, and they had sufficient bite force and tooth pressure to break apart chitin of appropriately sized prey. This suggests that they could have been generalist insectivores, but the differing morphological and biomechanical properties of the teeth of the two taxa suggest they had distinct diets. *C. hudsoni*X had much stouter, lenticular teeth with a greater bite force than *C. cambrica*, and lacked the pronounced escape structures upon its teeth, and is therefore inferred to have taken larger and harder prey items, which could have included small vertebrates. *C. cambrica*, despite its high bite pressure, had less robust teeth, with a much lower mechanical advantage in its anteriormost teeth, and relatively narrower skull, and so it may have specialized on smaller, faster prey items.

The last clevosaurs disappeared in the Early Jurassic, coinciding with the rising diversity of mammaliaforms and squamates following the end-Triassic extinction event. Our morphometric analysis shows that clevosaurs occupied a distinct region of morphospace from other rhynchocephalians, and this niche closed in the Early Jurassic and has remained unoccupied within the clade ever since. The Early Jurassic mammaliaforms and squamates were similarly sized vertebrates, predominantly insectivorous and would have shared a similar dietary niche to *Clevosaurus*. The teeth of *Clevosaurus* were probably functionally analogous to the shearing molariform teeth of early mammaliaforms, such as the precisely occluding teeth of *Morganucodon*. In addition, we speculate that the rhynchocephalians may have evolved their enlarged lateral row of palatine teeth parallel to the maxillary teeth as a functional equivalent to the multiscupid mammalian tooth, but at the cost of limited movement about their long axis. This was further exacerbated in *Clevosaurus* by the precise and deep occlusion between the teeth of the dentary and maxilla. Rhynchocephalians, as a whole, showed different morphologies between the Triassic and subsequent periods.

Further investigations could explore the biomechanical properties of mandibles of taxa that coexisted with mammaliaforms, including basal rhynchocephalians such as *Gephyrosaurus* in order to test more thoroughly whether, and to what extent, these early rhynchocephalians and mammaliaforms might have competed. The small vertebrates from the Triassic/Jurassic fissures in the Bristol Channel region provide a possible test case.

Acknowledgements. We thank Sandra Chapman (NHMUK) who has continually supported and encouraged this work, as well as Mike Day (NHMUK) who registered some of the specimens at short notice. We also thank Aileen O'Brien (University of Southampton, UK) and Emily Keeble (University of Bristol, UK) for acquiring the original CT scans and segmented surfaces of *Clevosaurus hudsoni* and *C. cambrica*, which were vital components for this work. We would also thank Tom Davies at the University of Bristol for the CT scans of *C. cambrica*, and Mark Mavrogordato and Kathryn Rankin at the University of Southampton for acquiring the CT scans of *C. hudsoni*. And finally, we acknowledge the Tratman Scholarship for funding the SAVC-T's PhD. We thank David Button (NHMUK) and an anonymous referee whose comments greatly improved this paper.

DATA ARCHIVING STATEMENT

The original CT-scan images for both specimens available on request from the Natural History Museum, London, UK. Additional data for this study are available in the Dryad Digital Repository: https://doi.org/10.5061/dryad.qjq2bvqcg

Editor. Stephan Lautenschlager

REFERENCES

ADAMS, D. C. and OTÁROLA-CASTILLO, E. 2013. geomorph: an R package for the collection and analysis of geometric morphometric shape data. *Methods in Ecology & Evolution*, **4**, 393–399.

ADAMS, N. F., RAYFIELD, E. J., COX, P. G., COBB, S. N. and CORFE, I. J. 2019. Functional tests of the competitive exclusion hypothesis for multituberculate extinction. *Royal Society Open Science*, **6**, 181536.

AGUIRRE, L. F., HERREL, A., VAN DAMME, R. and MATTHYSEN, E. 2003. The implications of food hardness for diet in bats. *Functional Ecology*, **17**, 201–212.

ANDERSON, P. S., FRIEDMAN, M., BRAZEAU, M. D. and RAYFIELD, E. J. 2011. Initial radiation of jaws demonstrated stability despite faunal and environmental change. *Nature*, **476**, 206–209.

—— —— and RUTA M. 2013. Late to the table: diversification of tetrapod mandibular biomechanics lagged behind the evolution of terrestriality. *Integrative & Comparative Biology*, **53**, 197–208.

APESTEGUÍA, S. 2005. Post-Jurassic sphenodontids: identity of the last lineages. 26–29. *In* KELLNER, A. W. A., HENRIQUES, D. D. R. and RODRIGUES, T. (eds). *Boletim de Resumos, II Congresso Latino-Americano de Paleontologia de Vertebrados*. Museu Nacional, Rio de Janeiro, 285 pp.

BONAPARTE, J. F. and SUES, H.-D. 2006. A new species of *Clevosaurus* (Lepidosauria: Rhynchocephalia) from the Upper Triassic of Rio Grande do Sul, Brazil. *Palaeontology*, **49**, 917–923.

CARTER, D. R. and BEAUPRÉ, G. S. 2001. *Skeletal function and form: Mechanobiology of skeletal development, aging, and regeneration*. Cambridge University Press, 318 pp.

CHAMBI-TROWELL, S. A. V., WHITESIDE, D. I. and BENTON, M. J. 2019. Diversity in rhynchocephalian *Clevosaurus* skulls based on CT reconstruction of two Late Triassic species from Great Britain. *Acta Palaeontologica Polonica*, **64**, 41–64.

—— —— —— and RAYFIELD E. J. 2020. Data from: Biomechanical properties of the jaws of two species of *Clevosaurus* and a reanalysis of rhynchocephalian dentary morphospace. *Dryad Digital Repository*. https://doi.org/10.5061/dryad.qjq2bvqcg

CORNETTE, R., TRESSET, A., HOUSSIN, C., PASCAL, M. and HERREL, A. 2015. Does bite force provide a competitive advantage in shrews? The case of the greater white-toothed shrew. *Biological Journal of the Linnean Society*, **114**, 795–807.

CREECH, J. 2004. Phylogenetic character analysis of crocodilian enamel microstructure and its relevance to biomechanical performance. Unpublished Masters thesis, Florida State University, Tallahassee.

CUFF, A. R. and RAYFIELD, E. J. 2013. Feeding mechanics in spinosaurid theropods and extant crocodilians. *PLoS One*, **8**, e65295.

CURREY, J. D. 1967. The failure of exoskeletons and endoskeletons. *Journal of Morphology*, **123**, 1–16.

—— 2002. *Bones: Structure and mechanics*. Princeton University Press, 456 pp.

CURTIS, N., JONES, M. E. H., EVANS, S. E., O'HIGGINS, P. and FAGAN, M. 2009. Visualising muscle anatomy using three-dimensional computer models – an example using the head and neck muscles of *Sphenodon*. *Palaeontologia Electronica*, **12** (3), art. 12.3.7T.

—— —— LAPPIN, A. K., O'HIGGINS, P., EVANS, S. E. and FAGAN, M. 2010. Comparison between *in vivo* and theoretical bite performance: using multi-body modelling to predict muscle and bite forces in a reptile skull. *Journal of Biomechanics*, **43**, 2804–2809.

—— —— O'HIGGINS, P., EVANS, S. E. and FAGAN, M. J. 2011. Functional relationship between skull form and feeding mechanics in *Sphenodon*, and implications for diapsid skull development. *PLoS One*, **6**(12), e29804.

DUMONT, E. R., GROSSE, I. R. and SLATER, G. J. 2009. Requirements for comparing the performance of finite element models of biological structures. *Journal of Theoretical Biology*, **256**, 96–103.

ERICKSON, G. M., LAPPIN, A. K. and VLIET, K. A. 2003. The ontogeny of bite-force performance in American alligator (*Alligator mississippiensis*). *Journal of Zoology*, **260**, 317–327.

—— GIGNAC, P. M., STEPPAN, S. J., LAPPIN, A. K., VLIET, K. A., BRUEGGEN, J. D., INOUYE, B. D., KLEDZIK, D. and WEBB, G. J.. 2012. Insights into the ecology and evolutionary success of crocodilians revealed through bite-force and tooth-pressure experimentation. *PLoS One*, **7**, e31781.

EVANS, S. E., PRASAD, G. V. R. and MANHAS, B. K. 2001. Rhynchocephalians (Diapsida: Lepidosauria) from the Jurassic Kota Formation of India. *Zoological Journal of the Linnean Society*, **133**, 309–334.

FRASER, N. C. 1988. The osteology and relationships of *Clevosaurus* (Reptilia: Sphenodontida). *Philosophical Transactions of the Royal Society B*, **321**, 125–178.

—— and WALKDEN, G. M. 1983. The ecology of a late Triassic reptile assemblage from Gloucestershire, England. *Palaeogeography, Palaeoclimatology, Palaeoecology*, **42**, 341–365.

GIGNAC, P. M. and ERICKSON, G. M. 2015. Ontogenetic changes in dental form and tooth pressures facilitate developmental niche shifts in American alligators. *Journal of Zoology*, **295**, 132–142.

GILL, P. G., PURNELL, M. A., CRUMPTON, N., BROWN, K. R., GOSTLING, N. J., STAMPANONI, M. and RAYFIELD, E. J. 2014. Dietary specializations and diversity in feeding ecology of the earliest stem mammals. *Nature*, **512**, 303–305.

GORNIAK, G. C., ROSENBERG, H. L. and GANS, C. 1982. Mastication in the tuatara, *Sphenodon punctatus* (Reptilia: Rhynchocephalia): structure and activity of the motor system. *Journal of Morphology*, **171**, 321–353.

GRÖNING, F., JONES, M. E. H., CURTIS, N., HERREL, A., O'HIGGINS, P. and FAGAN, M. 2013. The importance of accurate muscle modelling for biomechanical analyses: a case study with a lizard skull. *Journal of the Royal Society Interface*, **10**, 20130216.

HAMMER, Ø., HARPER, D. A. T. and RYAN, P. D. 2001. Paleontological statistics software: package for education and data analysis. *Palaeontologia Electronica*, **4**, 1–9.

HERREL, A., CASTILLA, A., AL-SULAITI, M. and WESSELS, J. 2013. Does large body size relax constraints on bite-force generation in lizards of the genus *Uromastyx*? *Journal of Zoology*, **292**, 170–174.

HERRERA-FLORES, J. A., STUBBS, T. L. and BENTON, M. J. 2017. Macroevolutionary patterns in Rhynchocephalia: is the tuatara (*Sphenodon punctatus*) a living fossil? *Palaeontology*, **60**, 319–328.

—— —— ELSLER, A. and BENTON, M. J. 2018. Taxonomic reassessment of *Clevosaurus latidens* Fraser, 1993 (Lepidosauria, Rhynchocephalia) and rhynchocephalian phylogeny based on parsimony and Bayesian inference. *Journal of Palaeontology*, **92**, 734–742.

HSIOU, A. S., GALLO DE FRANCA, M. A. and FERIGOLO, J. 2015. New data on the *Clevosaurus* (Sphenodontia: *Clevosauridae*) from the Upper Triassic of Southern Brazil. *PLoS One*, **10** (9), e0137523.

—— NYDAM, R. L., SIMÕES, T. R., PRETTO, F. A., ONARY, S., MARTINELLI, A. G., LIPARINI, A., ROMO DE VIVAR MARTÍNEZ, P., BENTO SOARES, M., SCHULTZ, C. L. and CALDWELL, M. W.

2019. A new clevosaurid from the Triassic (Carnian) of Brazil and the rise of sphenodontians in Gondwana. *Scientific Reports*, **9**, 11821.

JÄGER, K. K., GILL, P. G., CORFE, I. and MARTIN, T. 2019. Occlusion and dental function of *Morganucodon* and *Megazostrodon*. *Journal of Vertebrate Paleontology*, **39**, e1635135.

JONES, M. E. H. 2006. The Early Jurassic clevosaurs from China (Diapsida: Lepidosauria). *New Mexico Museum Natural History & Science Bulletin*, **37**, 548–562.

—— 2008. Skull shape and feeding strategy in *Sphenodon* and other Rhynchocephalia (Diapsida: Lepidosauria). *Journal of Morphology*, **269**, 945–966.

—— 2009. Dentary tooth shape in *Sphenodon* and its fossil relatives (Diapsida: Lepidosauria: Rhynchocephalia). *Frontiers of Oral Biology*, **13**, 9–15.

—— and LAPPIN, A. K. 2009. Bite-force performance of the last rhynchocephalian (Lepidosauria: *Sphenodon*). *Journal of the Royal Society of New Zealand*, **39**, 71–83.

—— CURTIS, N., O'HIGGINS, P., FAGAN, M. and EVANS, S. E. 2009. The head and neck muscles associated with feeding in *Sphenodon* (Reptilia: Lepidosauria: Rhynchocephalia). *Palaeontologia Electronica*, **12** (2), 12.2.7A.

—— ANDERSON, C. L., HIPSLEY, C. A., MÜLLER, J., EVANS, S. E. and SCHOCH, R. R. 2013. Integration of molecules and new fossils supports a Triassic origin for Lepidosauria (lizards, snakes, and tuatara). *BMC Evolutionary Biology*, **13**, 208.

KAMMERER, C. F., GRANDE, L. and WESTNEAT, M. W. 2006. Comparative and developmental functional morphology of the jaws of living and fossil gars (Actinopterygii: Lepisosteidae). *Journal of Morphology*, **267**, 1017–1031.

KEEBLE, E., WHITESIDE, D. I. and BENTON, M. J. 2018. The terrestrial fauna of the Late Triassic Pant-y-ffynnon Quarry fissures, South Wales, UK and a new species of *Clevosaurus* (Lepidosauria: Rhynchocephalia). *Proceedings of the Geologists' Association*, **129**, 99–119.

KIELAN-JAWOROSKA, Z., CIFELLI, R. and LUO, Z.-X. (eds). 2004. *Mammals from the age of dinosaurs*. Columbia University Press, 630 pp.

LAUTENSCHLAGER, S. 2013. Cranial myology and bite force performance of *Erlikosaurus andrewsi*: a novel approach for digital muscle reconstructions. *Journal of Anatomy*, **222**, 260–272.

LUCAS, P. W. and PETERS, C. R. 2007. Function of postcanine tooth crown shape in mammals. 282–289. *In* TEAFORD, M. F. (ed.) *Development, function, and evolution of teeth*. Cambridge University Press, 314 pp.

MAISANO, J. 2001. *Sphenodon punctatus,* Tuatara. *Digital Morphology*. http://digimorph.org/specimens/Sphenodon_punctatus/adult/

MELORO, C. and JONES, M. E. H. 2012. Tooth and cranial disparity in the fossil relatives of *Sphenodon* (Rhynchocephalia) dispute the persistent 'living fossil' label. *Journal of Evolutionary Biology*, **25**, 2194–2209.

MILNER, A. C., MILNER, A. R. and EVANS, S. E. 2000. Global changes and biota: amphibians, reptiles and birds. 316–332. *In* CULVER, S. and RAWSON, P. (eds). *Biotic response to global change: The last 145 million years*. Cambridge University Press, 398 pp.

MOAZEN, M., CURTIS, N., EVANS, S. E., O'HIGGINS, P. and FAGAN, M. 2008. Combined finite element and multibody dynamics analysis of biting in a *Uromastyx hardwickii* lizard skull. *Journal of Anatomy*, **213**, 499–508.

O'BRIEN, A., WHITESIDE, D. I. and MARSHALL, J. E. A. 2018. Anatomical study of two previously undescribed specimens of *Clevosaurus hudsoni* (Lepidosauria: Rhynchocephalia) from Cromhall Quarry, UK, aided by computed tomography, yields additional information on the skeleton and hitherto undescribed bones. *Zoological Journal of the Linnean Society*, **183**, 163–195.

R CORE TEAM. 2019. *R: a language and environment for statistical computing*. v.3.6.1. R Foundation for Statistical Computing. https://www.R-project.org

REYNOSO, V. H. 1997. A "beaded" sphenodontian (Diapsida: Lepidosauria) from the Early Cretaceous of central Mexico. *Journal of Vertebrate Paleontology*, **17**, 52–59.

ROBINSON, P. L. 1976. How *Sphenodon* and *Uromastix* grow their teeth and use them. 43–64. *In* BELLAIRS, A. D. A. and BOX, C. B. (eds). *Morphology and biology of reptiles*. Academic Press.

ROHLF, F. J. 2006. *tpsDig: digitize coordinates of landmarks and capture outlines. v. 2.10*. Department of Ecology & Evolution, State University of New York at Stony Brook. http://life.bio.sunysb.edu/morph

ROMO DE VIVAR MARTINEZ, P. R. and BENTO SOARES, M. 2015. Dentary morphological variation in *Clevosaurus brasiliensis* (Rhynchocephalia, Clevosauridae) from the Upper Triassic of Rio Grande do Sul, Brazil. *PLoS One*, **10** (3), e0119307.

SÄILÄ, L. K. 2005. A new species of the sphenodontian reptile Clevosaurus from the lower Jurassic of South Wales. *Palaeontology*, **48**, 817–831.

SANTANA, S., STRAIT, S. and DUMONT, E. 2011. The better to eat you with: functional correlates of tooth structure in bats. *Functional Ecology*, **25**, 839–847.

SCHAERLAEKEN, V., HERREL, A., AERTS, P. and ROSS, C. F. 2008. The functional significance of the lower temporal bar in *Sphenodon punctatus*. *Journal of Experimental Biology*, **211**, 3908–3914.

SOKOL, O. M. 1967. Herbivory in lizards. *Evolution*, **21**, 192–194.

STRAIT, D. S., WANG, Q., DECHOW, P. C., ROSS, C. F., RICHMOND, B. G., SPENCER, M. A. and PATEL, B. A. 2005. Modeling elastic properties in finite element analysis: how much precision is needed to produce an accurate model? *The Anatomical Record*, **283A**, 275–287.

STUBBS, T. L., PIERCE, S. E., RAYFIELD, E. J. and ANDERSON, P. S. 2013. Morphological and biomechanical disparity of crocodile-line archosaurs following the end-Triassic extinction. *Proceedings of the Royal Society B*, **280**, 20131940.

SUES, H.-D. and REISZ, R. R. 1995. First record of the early Mesozoic sphenodontian *Clevosaurus* (Lepidosauria: Rhynchocephalia) from the Southern Hemisphere. *Journal of Paleontology*, **69**, 123–126.

—— SHUBIN, N. H. and OLSEN, P. E. 1994. A new sphenodontian (Lepidosauria: Rhynchocephalia) from the McCoy Brook Formation (Lower Jurassic) of Nova Scotia, Canada. *Journal of Vertebrate Paleontology*, **14**, 327–340.

SWINTON, W. E. 1939. A new Triassic rhynchocephalian from Gloucestershire. *Annals & Magazine of Natural History*, **4**, 591–594.

TAYLOR, A. C., LAUTENSCHLAGER, S., QI, Z. and RAYFIELD, E. J. 2017. Biomechanical evaluation of different musculoskeletal arrangements in *Psittacosaurus* and implications for cranial function. *The Anatomical Record*, **300**, 49–61.

THOMASON, J. J. 1991. Cranial strength in relation to estimated biting forces in some mammals. *Canadian Journal of Zoology*, **69**, 2326–2333.

TSENG, Z. J., McNITT-GRAY, J. L., FLASHNER, H., WANG, X. and ENCISCO, R. 2011. Model sensitivity and use of the comparative finite element method in mammalian jaw mechanics: mandible performance in the gray wolf. *PLoS One*, **6**, e19171.

VERVUST, B., VAN DONGEN, S., GRBAC, I. and VAN DAMME, R. 2009. The mystery of the missing toes: extreme levels of natural mutilation in island lizard populations. *Functional Ecology*, **23**, 996–1003.

VERWAIJEN, D., VAN DAMME, R. and HERREL, A. 2002. Relationships between head size, bite force, prey handling efficiency and diet in two sympatric lacertid lizards. *Functional Ecology*, **16**, 842–850.

WHITESIDE, D. I. 1983. A fissure fauna from Avon. Unpublished PhD thesis, University of Bristol, 216 pp.

—— and DUFFIN, C. J. 2017. Late Triassic terrestrial microvertebrates from Charles Moore's '*Microlestes*' quarry, Holwell, Somerset, UK. *Zoological Journal of the Linnean Society*, **179**, 677–705.

—— —— GILL, P. G., MARSHALL, J. E. A. and BENTON, M. J. 2016. The Late Triassic and Early Jurassic fissure faunas from Bristol and South Wales: stratigraphy and setting. *Palaeontologia Polonica*, **67**, 257–287.

—— —— and FURRER H. 2017. The Late Triassic lepidosaur fauna from Hallau, North-Eastern Switzerland, and a new 'basal' rhynchocephalian *Deltadectes elvetica* gen et. sp. nov. *Neues Jahrbuch für Geologie und Paläontologie, Abhandlungen*, **285**, 53–74.

WU, X. C. 1994. Late Triassic-Early Jurassic sphenodontians from China and the phylogeny of the Sphenodontia. 38–69. *In* FRASER, N. C. and SUES, H.-D. (eds). *In the shadow of the dinosaurs*. Cambridge University Press, 448 pp.